


# Polar localization of a rice silicon transporter requires isoleucine at both C- and N-termini as well as positively charged residues

Noriyuki Konishi, Namiki Mitani-Ueno, Naoki Yamaji and Jian Feng Ma \*

Institute of Plant Science and Resources, Okayama University, Chuo 2-20-1, Kurashiki 710-0046, Japan

\*Author for correspondence: [maj@rib.okayama-u.ac.jp](mailto:maj@rib.okayama-u.ac.jp)

The author(s) responsible for distribution of materials integral to the findings presented in this article in accordance with the policy described in the Instructions for Authors (<https://academic.oup.com/plcell/>) is: Jian Feng Ma ([maj@rib.okayama-u.ac.jp](mailto:maj@rib.okayama-u.ac.jp)).

## Abstract

Silicon (Si) is important for stable and high yields in rice (*Oryza sativa*), a typical Si hyperaccumulator. The high Si accumulation is achieved by the cooperation of 2 Si transporters, LOW SILICON 1 (OsLsi1) and OsLsi2, which are polarly localized in cells of the root exodermis and endodermis. However, the mechanism underlying their polar localization is unknown. Here, we identified amino acid residues critical for the polar localization of OsLsi1. Deletion of both N- and C-terminal regions resulted in the loss of its polar localization. Furthermore, the deletion of the C-terminus inhibited its trafficking from the endoplasmic reticulum to the plasma membrane. Detailed site-directed mutagenesis analysis showed that Ile18 at the N-terminal region and Ile285 at the C-terminal region were essential for the polar localization of OsLsi1. Moreover, a cluster of positively charged residues at the C-terminal region is also required for polar localization. Phosphorylation and Lys modifications of OsLsi1 are unlikely to be involved in its polar localization. Finally, we showed that the polar localization of OsLsi1 is required for the efficient uptake of Si. Our study not only identified critical residues required for the polar localization of OsLsi1, but also provided experimental evidence for the importance of transporter polarity for efficient nutrient uptake.

## Introduction

Plants require 14 mineral nutrients for their growth and development. Mineral nutrients from the soil solution must be transported across several root cell layers to the central cylinder of the roots for translocation to the above-ground parts of the plant (Barberon and Geldner 2014; Che et al. 2018; Huang et al. 2020). Three different pathways have been proposed for the uptake of mineral nutrients: the apoplastic pathway, symplastic pathway, and transcellular pathway (Barberon and Geldner 2014). Due to the presence of Casparian strips (CS) acting as a physical barrier for an apoplastic route, the contribution of the apoplastic pathway to mineral uptake is limited compared with the symplastic and transcellular pathways, which require both influx and efflux transporters for entering and exiting root cells (Barberon and Geldner 2014).

Some mineral transporters show polar localization in different plant species (Gordon-Weeks et al. 2003; Ma et al. 2006, 2007; Takano et al. 2010; Kiba et al. 2012; Sasaki et al. 2012; Barberon et al. 2014; Ueno et al. 2015; Konishi and Ma 2021; Guo et al. 2022; Huang et al. 2022). The polar localization of these transporters has been proposed to play an important role in the efficient and directional uptake of mineral elements, but the mechanisms underlying the polar localization are largely unknown. In *Arabidopsis* (*Arabidopsis thaliana*), the transporters NOD26-LIKE INTRINSIC PROTEINS5;1 (AtNIP5;1) and BORON TRANSPORTER1 (AtBOR1) involved in boron (B) uptake show polar localization. AtNIP5;1 is polarly localized at the distal side of root cells, while AtBOR1 is at the proximal side (Takano et al. 2010).

Clathrin-mediated endocytosis (CME) is required for the polar localization of these transporters (Alassimone et al. 2010;

## IN A NUTSHELL

**Background:** Silicon (Si) is a beneficial element for plants. Rice (*Oryza sativa*) can accumulate Si in shoots up to 10% of dry weight; this accumulation helps alleviate various stresses and is essential for stable and high production of rice. The high Si accumulation in rice is achieved by the cooperation of 2 Si transporters, LOW SILICON 1 and 2 (OsLsi1 and OsLsi2) expressed in the roots. OsLsi1, a channel-type transporter, is present in the plasma membrane of the root exodermis and endodermis and localizes to the outer side of the cell toward the soil (distally localized). OsLsi2, an efflux-type transporter, is oppositely localized at the inner side (proximally localized) of the same cells. OsLsi1 and OsLsi2 form an efficient pathway for Si uptake in rice roots.

**Question:** What is the mechanism underlying the polar localization of these transporters? How important is the polar localization in efficient Si uptake?

**Findings:** With deletion and site-directed mutation approaches, we identified the critical amino acid residues required for the polar localization of OsLsi1. They are Ile18, Ile285, and positively charged residues from the N- and C-terminal cytosolic regions of OsLsi1. Interestingly, phosphorylation, ubiquitination, and clathrin-mediated endocytosis are not involved in the polar localization. Furthermore, comparing Si uptake between plants carrying polar or nonpolar OsLsi1 variants showed that polar localization of OsLsi1 plays a significant role in efficient Si uptake.

**Next steps:** The factors that interact with OsLsi1 for its polar localization remain to be determined. Other mechanisms involved in the polar localization of mineral element transporters also need to be investigated, especially in crops such as rice.

Yoshinari et al. 2016, 2019; Wang et al. 2017). When CME is suppressed by an inhibitor or dominant-negative expression of a loss-of-function variant of DYNAMIN-RELATED PROTEIN1A (DRP1A), which requires cleaving of the clathrin-coated vesicle from the plasma membrane, AtNIP5;1 and AtBOR1 lost their polar localization (Alassimone et al. 2010; Yoshinari et al. 2016). Knockout mutants of mu or sigma subunit of the ADAPTOR PROTEIN2 (AP2) complex, which is one of the components in the CME pathways, also resulted in the loss of polar localization of AtNIP5;1 and AtBOR1, indicating that AP2-dependent CME is required for their polar localization (Wang et al. 2017; Yoshinari et al. 2019). Further studies showed that the AP2 complex could directly bind with the C-terminus of the AtBOR1 (Yoshinari et al. 2019), while the N-terminus of AtNIP5;1 might interact with the AP2 complex through phosphorylated N-terminal TPG repeat, which is required for polarity maintenance via constitutive endocytosis (Wang et al. 2017).

In contrast to transporters whose localization requires CME, the polar localization of IRON REGULATED TRANSPORT1 (AtIRT1), a ferrous iron (Fe) transporter showing polar localization at the distal side of the root epidermal cell, is maintained when CME was inhibited through a dominant-negative expression of the clathrin hub (Barberon et al. 2014). Instead, its polar localization is controlled by a PHOSPHATIDYLINOSITOL-3-PHOSPHATE-BINDING PROTEIN RECRUITED TO LATE ENDOSOMES through direct interaction with the cytosolic loop of AtIRT1 (Barberon et al. 2014).

The mechanisms for polar localization of transporters in rice (*Oryza sativa*) remain unclear, although several transporters have been reported to show polar localization. Two transporters involved in silicon (Si) uptake, LOW SILICON 1

(OsLsi1) and OsLsi2, are polarly localized at the distal and proximal side, respectively, of both root exodermis and endodermis (Ma et al. 2006, 2007). Similarly, NATURAL RESISTANCE-ASSOCIATED MACROPHAGES5 (OsNramp5) and METAL TOLERANCE PROTEIN 9 (OsMTP9), involved in manganese (Mn) uptake, and OsLsi1 and OsBOR1, involved in B uptake, also show polar localization in rice roots (Sasaki et al. 2012; Ueno et al. 2015; Shao et al. 2018; Huang et al. 2022). These transporters form a cooperative system for the efficient uptake of mineral elements through a pair of influx–efflux transporters at the exodermis and endodermis (Ma and Yamaji 2015; Che et al. 2018; Huang et al. 2020). Knockout of either of them resulted in a significant reduction in uptake (Ma et al. 2006, 2007; Sasaki et al. 2012; Ueno et al. 2015; Shao et al. 2018; Huang et al. 2022). This distinct uptake system in rice has been attributed to the unique root anatomy, which is characterized by 2 CS at the exodermis and endodermis and the formation of aerenchyma in the cortex (Enstone et al. 2002).

A recent study showed that, unlike in Arabidopsis, CME is unlikely to be involved in the polar localization of OsLsi1, OsLsi2, and OsBOR1 in Si and B uptake in rice (Huang et al. 2022; Konishi et al. 2022). This is supported by the finding that the polar localization of OsLsi1, OsLsi2, and OsBOR1 is unaffected by a dominant-negative induction of loss-of-function OsDRP1A variant and by knockout of the mu subunit of the AP2 complex (Huang et al. 2022; Konishi et al. 2022). These observations suggest that the polar localization of mineral element transporters is regulated by different mechanisms in rice and Arabidopsis.

In this study, we investigated the mechanism underlying the polar localization of OsLsi1 in rice. OsLsi1 is a channel-type transporter of Si, which belongs to the aquaporin

Nod26-like intrinsic protein (NIP) III subfamily (Ma et al. 2006; Mitani et al. 2008). It is responsible for the influx transport of Si in the form of silicic acid from soil solution to the exodermis cells and further from the apoplastic space in the aerenchyma to the endodermis cells (Ma et al. 2006). Knockout of this gene significantly reduced Si uptake and accumulation, resulting in great loss of yield because high Si accumulation in the above-ground parts (leaves and husk) is required for the healthy growth of rice by alleviating various stresses (Ma et al. 2006). OsLsi1 also shows transport activity for arsenite, boric acid, and selenite due to their similar chemical properties to silicic acid (Ma et al. 2008; Zhao et al. 2010; Mitani-Ueno et al. 2011; Shao et al. 2018). Unlike other aquaporins, OsLsi1 shows distinctive transmembrane helical orientations, which is characterized by a unique, widely opened, and hydrophilic selectivity filter composed of 5 residues (Saitoh et al. 2021). Its homologs have been identified in other plant species, including HvLsi1 in barley (*Hordeum vulgare*, Chiba et al. 2009), TaLsi1 in wheat (*Triticum aestivum*, Montpetit et al. 2012), CsLsi1 in cucumber (*Cucumis sativus*, Sun et al. 2017), ZmLsi1 in maize (*Zea mays*, Mitani et al. 2009), CmLsi1 in pumpkin (*Cucurbita moschata*, Mitani et al. 2011), VvLsi1 in grape (*Vitis vinifera*, Noronha et al. 2020), and SLsi1 in tomato (*Solanum lycopersicum*, Sun et al. 2020). Among them, HvLsi1 in barley, ZmLsi1 in maize, and CsLsi1 in cucumber show polar localization (Chiba et al. 2009; Mitani et al. 2009; Sun et al. 2017), while CmLsi1 in pumpkin and SLsi1 in tomato show nonpolar localization (Mitani et al. 2011; Sun et al. 2020). However, the mechanisms responsible for the polar localization of OsLsi1 and its orthologs are unclear. In the present study, we identified critical amino acid residues required for trafficking and the polar localization of OsLsi1 through deletion and site-directed mutagenesis. We also demonstrated that the polar localization of OsLsi1 is required for the efficient uptake of Si in rice.

## Results

### Both N- and C-terminal regions of OsLsi1 are involved in its polar localization

OsLsi1 has a large cytosolic region in the N- and C-terminus according to its crystal structure (Saitoh et al. 2021; Fig. 1A). To investigate whether N- or C-terminal region is required for the polar localization, we generated transgenic rice plants carrying Flag-tagged OsLsi1 (Flag-OsLsi1) with deletion of the N- and C-terminal regions under the control of *OsLsi1* promoter in the background of *lsi1-3* mutant defective in Si uptake (Chiba et al. 2009; Fig. 1A). Full-length Flag-OsLsi1 is functional in Si uptake and shows polar localization at the distal side of both exodermis and endodermis, as observed in native OsLsi1 in wild-type rice (Huang et al. 2022; Fig. 1B). Immunostaining using anti-Flag antibody showed that deletion of the N-terminal from the position of 2 to 40 did not affect the polar localization at all (Fig. 1C), while deletion of the C-terminal from 265 to 298 and deletion of

both N- and C-terminal regions resulted in accumulation of the signal in the intracellular organelles and surrounding the cell (Fig. 1, D and E).

To confirm whether the polarity of OsLsi1 was lost in these transgenic lines, we performed double immunostaining using markers of the plasma membrane. The result showed that the signal of Flag-OsLsi1<sup>d265–298</sup> overlapped well with the signal of OsNramp5, an Mn/cadmium transporter localized at the distal side of the plasma membrane (Sasaki et al. 2012), although the intracellular signal did not overlap (Supplemental Figs. S1A and D). On the other hand, the signal did not overlap with the OsBOR1 signal, a B transporter localized at the proximal side of the plasma membrane (Huang et al. 2022; Supplemental Fig. S1, B and E), indicating that the polar localization of OsLsi1 without the C-terminal region was maintained on the plasma membrane. By contrast, the signal of OsLsi1 without both N- and C-terminal regions overlapped with both OsNramp5 and OsBOR1, indicating that its polarity was lost (Supplemental Fig. S2, A–D). Taken together, these results suggest that either the N- or C-terminal region is sufficient to generate polar localization of OsLsi1 in rice roots.

### The C-terminal region of OsLsi1 contains a motif required for trafficking from the endoplasmic reticulum (ER) to plasma membrane

To identify the subcellular localization of intracellular signal observed in the transgenic line carrying *Flag-OsLsi1*<sup>d265–298</sup> together with the plasma membrane (Fig. 1D), we performed a double immunostaining with an ER marker, HDEL (Napier et al. 1992). The result showed that the intracellular signal of Flag-OsLsi1<sup>d265–298</sup> overlapped with the HDEL signal (Supplemental Figs. S1, C and F), indicating that part of OsLsi1 was accumulated in the ER due to the C-terminal deletion.

To narrow down the motif required for the trafficking of OsLsi1, we generated transgenic rice lines with various deletions of the C-terminal region (Supplemental Fig. S3A). Deletion of amino acids 265 to 281 and 282 to 289 did not affect the trafficking of OsLsi1, whereas deletion of amino acids 282 to 298 and 290 to 298 impaired the trafficking (Supplemental Fig. S3B–E). Taken together, our results show that the region of 290 to 298 at the C-terminal region is required for the trafficking of OsLsi1.

To confirm whether this narrowed region is sufficient for OsLsi1 trafficking, this motif with 2 additional residues from 288 to 298 (DDVDEMENIQV) was fused to C-terminal deleted OsLsi1, Flag-OsLsi1<sup>d265–287</sup> (Supplemental Fig. S4A). Flag-OsLsi1<sup>d265–287</sup> showed clear polar localization at the plasma membrane without any intracellular accumulations (Supplemental Fig. S4B), indicating that this motif is sufficient for OsLsi1 trafficking from the ER. When the N-terminal region was also deleted together with the C-terminal region from 265 to 287, similar to the result from Flag-OsLsi1<sup>d2–40, d265–298</sup>, the polar localization of Flag-OsLsi1<sup>d2–40, d265–287</sup> was impaired (Supplemental Fig. S4C). These observations indicated that

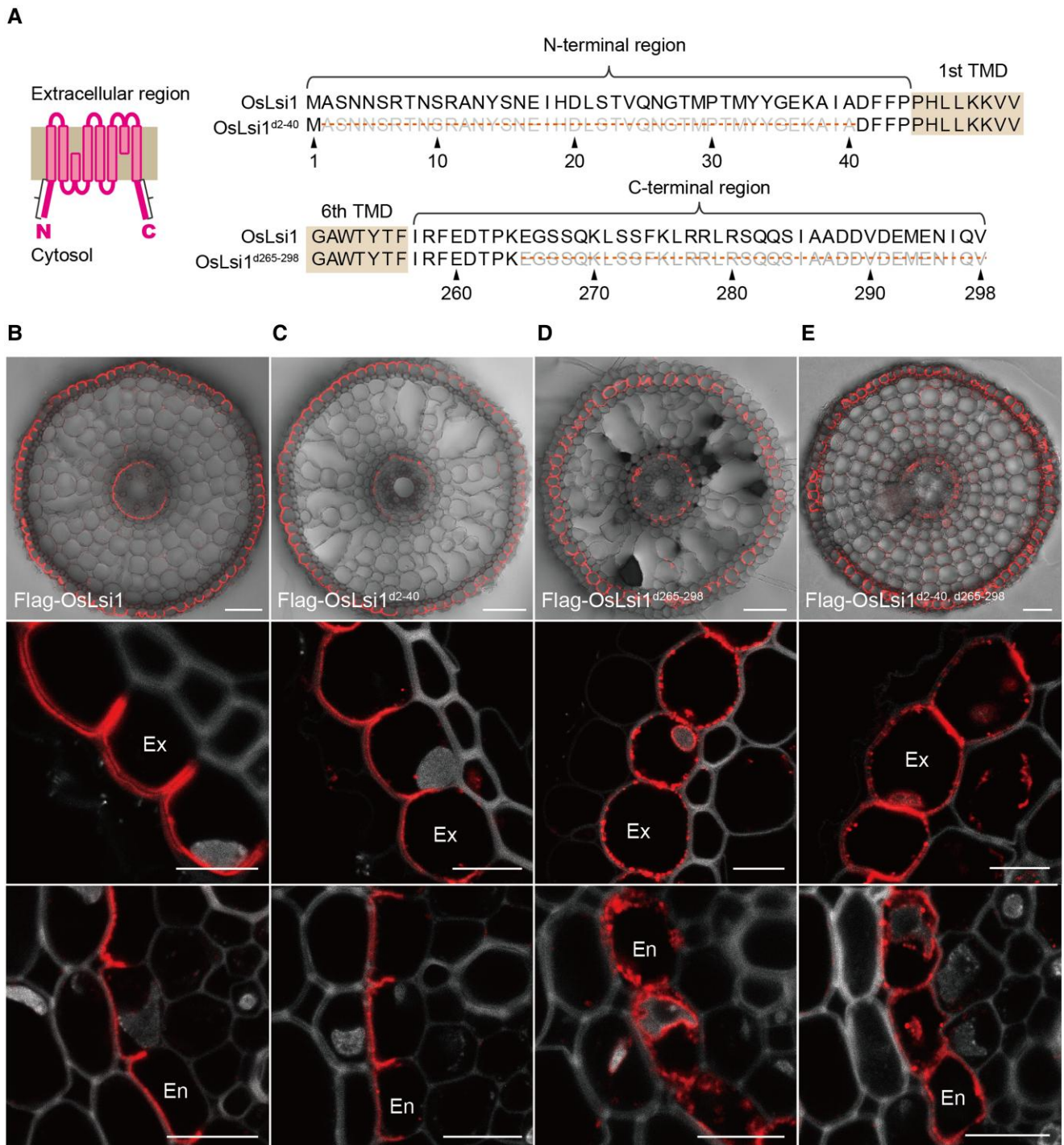


**Figure 1.** Role of N- and C-terminal regions in polar localization of OsLsi1. **A**) Scheme for OsLsi1 structure and deletion region of OsLsi1. The deletion regions at the N- and C-termini are indicated in orange lines. TMD indicates the transmembrane domain. **B to E**) Localization of OsLsi1 variants in roots. Localization of Flag-OsLsi1 **B**), Flag-OsLsi1<sup>d2-40</sup> **C**), Flag-OsLsi1<sup>d265-298</sup> **D**), and Flag-OsLsi1<sup>d2-40, d265-298</sup> **E**) in roots of transgenic lines. Cross-sections of the mature region (15 to 20 mm from the root tip) of the crown roots were used for immunostaining with an antibody against Flag-tag. Exodermis (Ex) and endodermis (En) were enlarged in the middle or lower panel, respectively **B**) to **E**). Red color indicates the signal of immunostained Flag-tagged proteins. Scale bars indicate 50  $\mu\text{m}$  in the whole root picture or 10  $\mu\text{m}$  in the enlarged picture **B**) to **E**).

the region between 288 and 298 is required for OsLsi1 trafficking but not for the polarity. In the subsequent experiments on the polar localization of OsLsi1, this motif from 288 to 298 was used to all C-terminal deleted constructs.

### The C-terminal region of OsLsi1 is sufficient for polar localization of the nonpolar aquaporin, OsNIP1;1

To further confirm whether the C- or N-terminal region is sufficient for generating polar localization, we prepared

chimeric proteins between OsLsi1 and OsNIP1;1 by swapping their C- and N-terminal regions (Fig. 2A; Supplemental Fig. S5A). OsNIP1;1 also belongs to NIP-type aquaporin and is implicated in As accumulation in rice (Sun et al. 2018). Different from OsLsi1, it does not show polar localization in rice roots (Sun et al. 2018). When Flag-tagged OsNIP1;1 was expressed under the control of the *OsLsi1* promoter in the *lsi1-3* mutant background, it showed nonpolar localization at both the exodermis and endodermis (Fig. 2B). By contrast, when the OsLsi1 C-terminus was fused to OsNIP1;1 without its own C-terminus, a clear polar localization was observed in both the endodermis and exodermis (Fig. 2C). However, a fusion of OsLsi1 N-terminal region to OsNIP1;1 without its own N-terminal region resulted in mislocalization of this chimera protein in other organelles rather than the plasma membrane (Supplemental Fig. S5B), suggesting that other unknown processes were affected due to swapping of N-terminal region. These findings further support that the C-terminal region of OsLsi1 is sufficient to generate polar localization for NIP-type aquaporins.

### Identification of polarity regulation region of the C- and N-termini of OsLsi1

To narrow down the region required for the polar localization of OsLsi1 at the C-terminus, we generated various transgenic lines harboring different regions of the OsLsi1 C-terminus fused to the C-terminus-deleted OsNIP1;1 (Fig. 2A). Furthermore, to quantify the polar localization, we calculated the polarity index based on the ratio of signal intensity at the distal and proximal sides of the cells (Supplemental Figs. S6A and B). If a transporter shows polar localization at the distal side, the index will be close to 1, as seen in Flag-OsNIP1;1<sup>dc</sup>-OsLsi1C and Flag-OsLsi1 (Fig. 2G; Supplemental Fig. S6A). If a transporter shows nonpolar localization, this value will be close to 0, as seen in Flag-OsNIP1;1 and Flag-OsLsi1<sup>d2-40, d265-287</sup> (Fig. 2G; Supplemental Fig. S6B). When the position of 288 to 298 at the C-terminus of OsLsi1 was fused to C-terminus-deleted OsNIP1;1, this chimeric protein (Flag-OsNIP1;1<sup>dc</sup>-OsLsi1C<sup>288-298</sup>) showed nonpolar localization (Supplemental Fig. S2, D and G). By contrast, fusion with the 282 to 298 region (Flag-OsNIP1;1<sup>dc</sup>-OsLsi1C<sup>282-298</sup>) gave clear polar localization to OsNIP1;1 at the endodermis, whereas it only gave a partial polarity at the exodermis (Fig. 2, E and G). However, a fusion of the 275 to 298 region (Flag-OsNIP1;1<sup>dc</sup>-OsLsi1C<sup>275-298</sup>) gave a clear polarity to OsNIP1;1 at both the endodermis and exodermis (Fig. 2, F and G). These results indicate that the position between 275 and 287 was crucial for polar localization at the C-terminus of OsLsi1.

To narrow down the N-terminus region responsible for the polarity, we also generated transgenic lines carrying different deletions in the N-terminus of the C-terminal deleted-OsLsi1 (OsLsi1<sup>d265-287</sup>) in the *lsi1-3* mutant background (Fig. 3A). Deletion of the 1 to 10 region at the N-terminus did not affect the polar localization of OsLsi1 (Fig. 3, B and E), whereas deletions of 1 to 20 and 1 to 30 regions resulted in decreased

polarity in both the exodermis and endodermis with less extent (Fig. 3, C–E). These results indicate that the region between 11 and 20 is important for polar localization of OsLsi1 at the N-terminus.

### Phosphorylation and Lys modifications are not involved in the polar localization of OsLsi1

In the narrowed-down region of both N- and C-termini, there are potential phosphorylation sites, including Tyr14 and Ser15 at the N-terminal region and Ser281 and Ser284 at the C-terminal region. To investigate whether phosphorylation of these residues is involved in the polar localization, we performed site-directed mutagenesis by substituting these residues with Ala to mimic nonphosphorylation in Flag-OsNIP1;1<sup>dc</sup>-OsLsi1C or Flag-OsLsi1<sup>d265-287</sup> (Fig. 4, A and C). However, these substitutions at both C- and N-termini did not affect the polar localization of the chimera protein and OsLsi1 (Fig. 4, D, H, and I). Furthermore, when Ser281 and Ser284 at the C-terminal region were substituted with Gln or Glu to mimic nonphosphorylation or phosphorylation (Fig. 4B), the polar localization of N-terminal deleted OsLsi1 was also not affected (Fig. 4, F, G, and I). These results indicate that phosphorylation is not involved in the polar localization of OsLsi1.

In addition, in the narrowed-down region of the C-terminus, there is a Lys residue, Lys275, which has the potential for modifications such as ubiquitination and sumoylation (Millar et al. 2019). To exclude the possibility that neighborhood Lys become a redundant target for these modifications, the 2 Lys residues, Lys270 and Lys275, were substituted with Arg in OsNIP1;1<sup>dc</sup>-OsLsi1C chimera protein (Fig. 4A). However, these substitutions did not affect the polar localization (Fig. 4, E and I). Taken together, it is unlikely that phosphorylation and Lys modifications are involved in the regulation of the polar localization of OsLsi1.

### Identification of crucial amino acid residues at the C-terminus required for the polar localization

To further identify the amino acid residues critical for the polar localization of OsLsi1 at the C-terminus, we performed a site-directed mutagenesis analysis. To do this, we generated transgenic lines carrying different mutations in N-terminal deleted OsLsi1. Based on the narrowed region shown above (Fig. 2), we first substituted 8 amino acids except for Ser, Lys, and Ala residues, at 276 to 280, 282 to 283, and 285 with Ala (Fig. 5A). As a result, the polarity index was decreased at both the exodermis and endodermis with less extent (Fig. 5, B and I). Substitution of amino acids at 276 to 280 partially decreased the polarity index at the exodermis but not at the endodermis (Fig. 5, C and I). Substitution of 282 to 283 and 285 with Ala resulted in decreased polarity index in the exodermis and endodermis with less extent (Fig. 5, D and I). Substitutions of Leu276 and 279 or Gln282 and 283 with Ala did not affect the polarity index (Fig. 5, E, G, and I), while substitutions of Arg277, 278, and 280 decreased the polarity index only at the exodermis but not at the

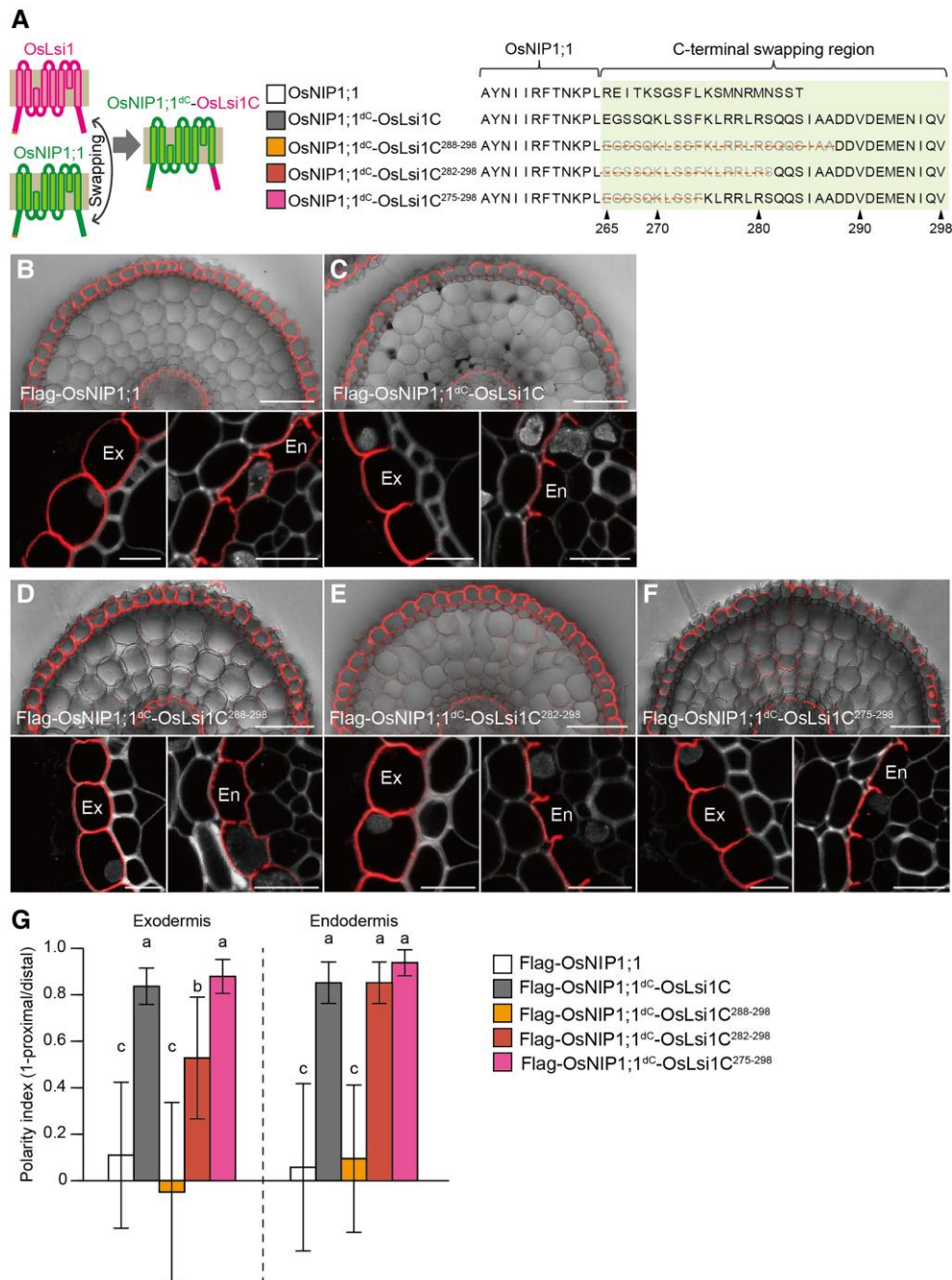


**Figure 2.** Role of C-terminal region of OsLsi1 in generating polar localization. **A)** Scheme representation for generating chimera proteins between OsLsi1 and OsNIP1;1. Magenta color shows OsLsi1, while green color shows OsNIP1;1. Orange lines on the right side show deleted region at the C-terminus of OsLsi1. **B to F)** Localization of chimera proteins between OsLsi1 and OsNIP1;1 in rice roots. Localization of Flag-OsNIP1;1 **B)**, Flag-OsNIP1;1<sup>dC</sup>-OsLsi1C **C)**, Flag-OsNIP1;1<sup>dC</sup>-OsLsi1C<sup>288–298</sup> **D)**, Flag-OsNIP1;1<sup>dC</sup>-OsLsi1C<sup>282–298</sup> **E)**, and Flag-OsNIP1;1<sup>dC</sup>-OsLsi1C<sup>275–298</sup> **F)** in roots of transgenic lines. Cross-sections of the mature region (15 to 20 mm from the root tip) of the crown roots were sampled for immunostaining. Red color indicates the signal of immunostained Flag-tagged proteins. Exodermis (Ex) and endodermis (En) in **B) to F)** were enlarged in the left or right of the lower half panel, respectively. Scale bars indicate 50  $\mu\text{m}$  in the whole root picture or 10  $\mu\text{m}$  in the enlarged picture. **G)** Polarity index of various Flag-OsNIP1;1<sup>dC</sup>-OsLsi1C variants shown in **B) to F)** at exodermis and endodermis. Thirty independent cells from more than 5 independent root slices were used for the quantification of the polarity index. Vertical bars indicate sd. Different letters indicate significant differences at  $P < 0.05$  by Tukey–Kramer’s test.

endodermis (Fig. 5, F and I). Furthermore, the substitution of Ile285 with Ala decreased the polarity in the exodermis and endodermis with less extent (Fig. 5, H and I). Taken together,

these results indicate that Ile285 and 3 Arg residues at 277, 278, and 280 in the C-terminus of OsLsi1 are required for its polarity.

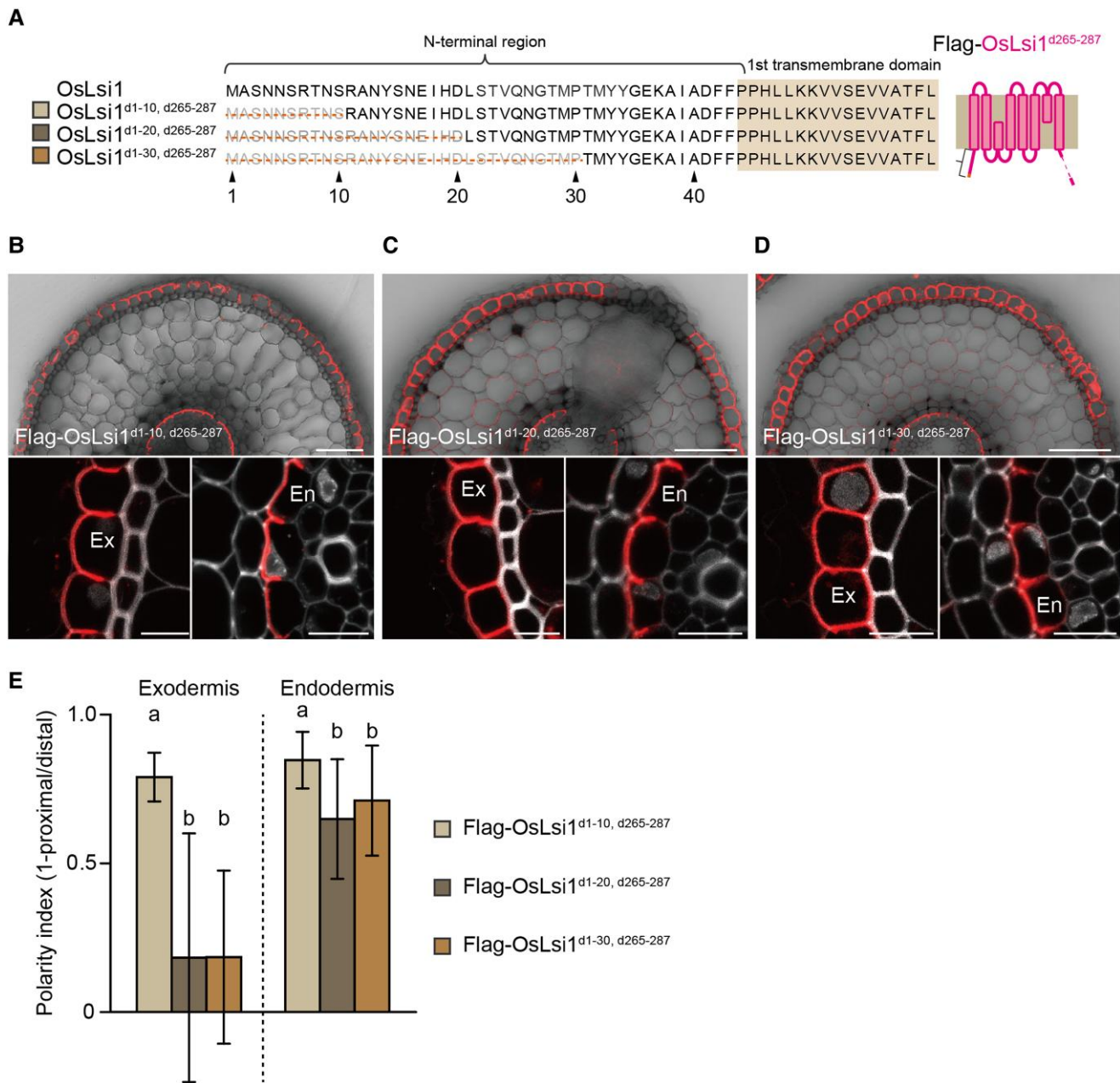


**Figure 3.** Identification of critical region at the N-terminal for polar localization of OsLsi1. **A)** Scheme presentation for the N-terminal deletion regions of Flag-OsLsi1<sup>d265–287</sup>. Orange lines show deleted regions. **B to D)** Localization of Flag-OsLsi1<sup>d1–10, d265–287</sup> **B)**, Flag-OsLsi1<sup>d1–20, d265–287</sup> **C)**, and Flag-OsLsi1<sup>d1–30, d265–287</sup> **D)** in roots of transgenic lines. Cross-sections of the mature region (15 to 20 mm from the root tip) of the crown roots of transgenic seedlings carrying deletion variants of *Flag-OsLsi1*<sup>d265–287</sup> were sampled for immunostaining. Red color indicates the signal of immunostained Flag-tagged proteins. Exodermis (Ex) and endodermis (En) in **B) to D)** were enlarged in the left or right of the lower half panel, respectively. Scale bars indicate 50  $\mu\text{m}$  in the whole root picture or 10  $\mu\text{m}$  in the enlarged picture. **E)** Polarity index of N-terminal deleted variants of Flag-OsLsi1<sup>d265–287</sup> shown in **B) to D)** at exodermis and endodermis. Thirty independent cells from more than 5 independent root slices were used for the quantification of the polarity index. Vertical bars indicate sd. Different letters indicate significant differences at  $P < 0.05$  by Tukey–Kramer’s test.

To further investigate which Arg residue is important to the polarity, each Arg residue was substituted to Ala in N-terminal deleted-OsLsi1 (Fig. 6A). All single substituted variants showed clear polar localization at both the exodermis and endodermis (Fig. 6, B–D, H). This result suggests that a cluster of Arg is

important for polar localization. Since Arg is positively charged, to test whether this amino acid feature is required for the polar localization, we substituted 3 Arg residues with Lys, which is also a positively charged residue (Fig. 6A). Unlike neutral charged-Ala substitution, these substitutions

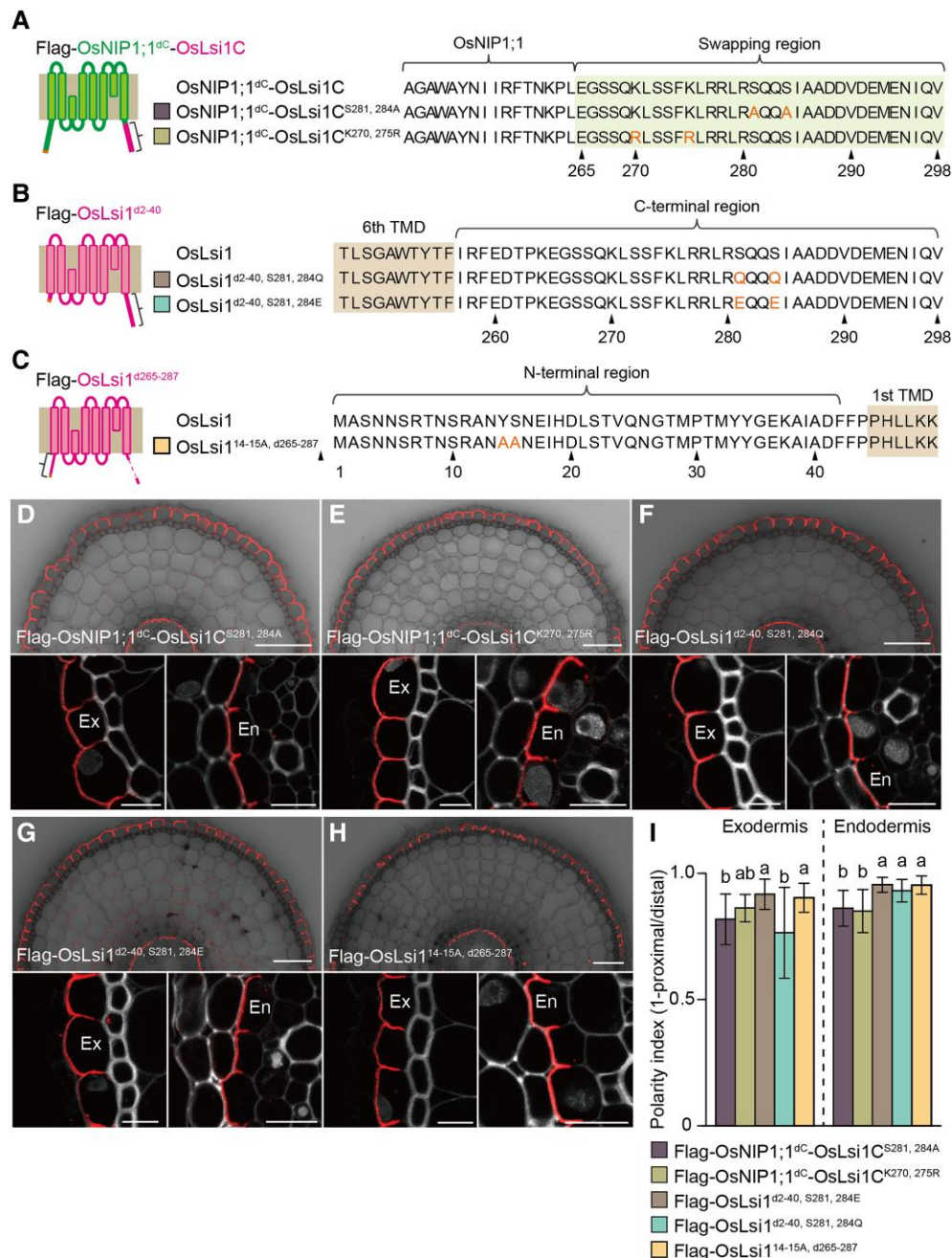


**Figure 4.** Possible involvement of phosphorylation and Lys modifications in polar localization of OsLsi1. **A to C**) Scheme presentation of substitution sites of Flag-OsNIP1;1<sup>dC</sup>-OsLsi1C **A**), Flag-OsLsi1<sup>d2-40</sup> **B**), and Flag-OsLsi1<sup>d265-287</sup> **C**). Orange letters show amino acids substituted. TMD indicates the transmembrane domain. **D to H**) Localization of Flag-OsNIP1;1<sup>dC</sup>-OsLsi1C<sup>S281, 284A</sup> **D**), and Flag-OsNIP1;1<sup>dC</sup>-OsLsi1C<sup>K270, 275R</sup> **E**), Flag-OsLsi1<sup>d2-40, S281, 284Q</sup> **F**), Flag-OsLsi1<sup>d2-40, S281, 284E</sup> **G**), and Flag-OsLsi1<sup>14-15A, d265-287</sup> **H**) in roots of transgenic lines. Cross-sections of the mature region (15 to 20 mm from the root tip) of the crown roots sampled from transgenic seedlings carrying different variants of *OsNIP1;1<sup>dC</sup>-OsLsi1C*, and *Flag-OsLsi1* were subjected to immunostaining using anti-Flag antibody. Exodermis (Ex) and endodermis (En) in **D**) to **H**) were enlarged in the left or right of the lower half panel, respectively. Scale bars indicate 50  $\mu$ m in the whole root picture or 10  $\mu$ m in the enlarged picture. **I**) Polarity index of various Flag-OsNIP1;1<sup>dC</sup>-OsLsi1C and Flag-OsLsi1 variants at the exodermis and endodermis. Thirty independent cells from more than 5 independent root slices were used for the quantification of the polarity index. Vertical bars indicate SD. Different letters indicate significant differences at  $P < 0.05$  by Tukey–Kramer’s test.

did not affect the polar localization (Fig. 6, E, F, and H). This observation indicates that positively charged amino acid residues are crucial for the polar localization of OsLsi1.

To investigate whether other positively charged residues at the C-terminus also have an influence on the polarity, Lys264, Lys270, and Lys275 were substituted to Ala together



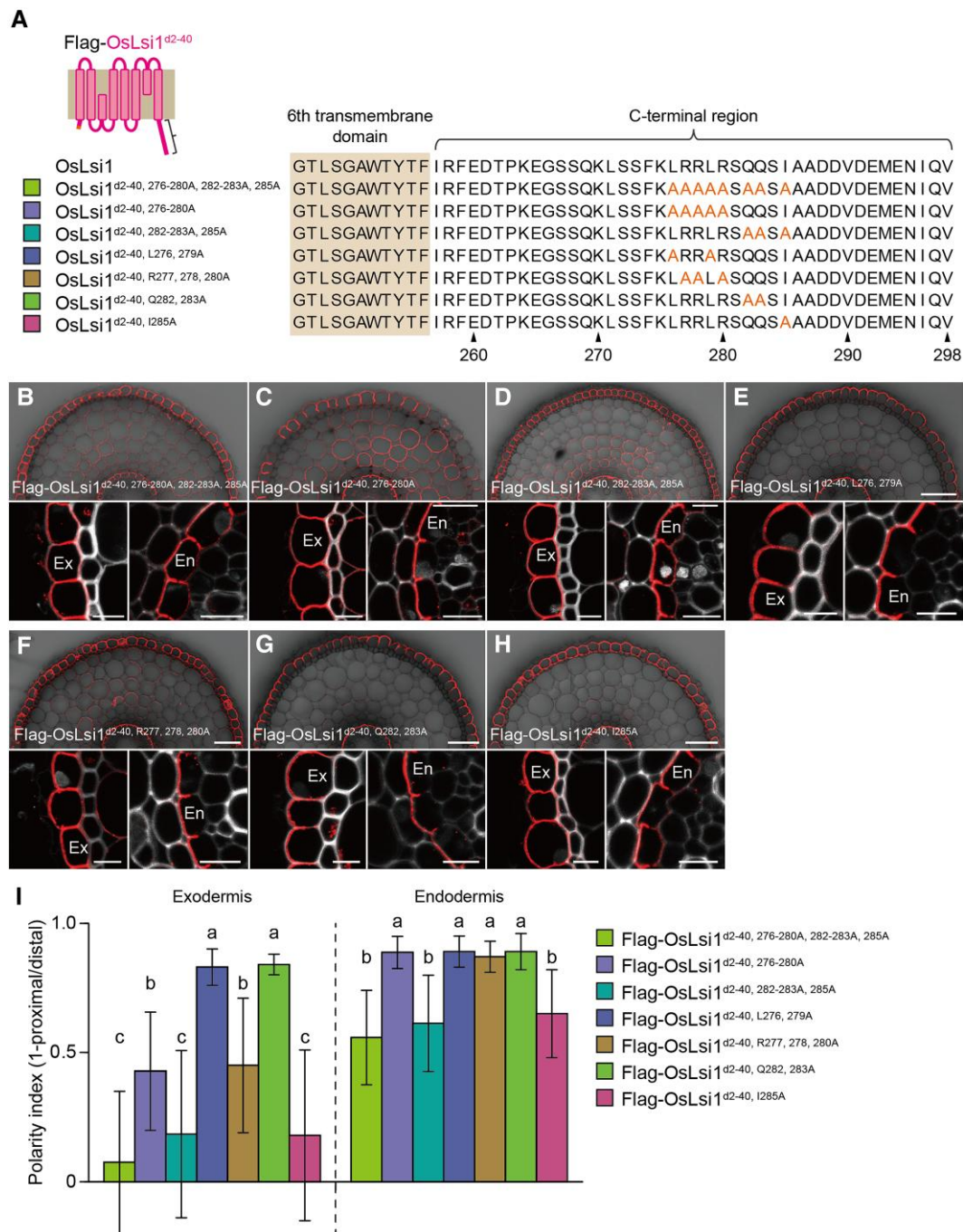


**Figure 5.** Identification of critical amino acids at the C-terminal region for polar localization of OsLsi1. **A)** Scheme presentation for substitution sites of the C-terminal region of Flag-OsLsi1<sup>d2-40</sup>. Orange letters show amino acids substituted. **B to I)** Localization of Flag-OsLsi1<sup>d2-40, 276-280A, 282-283A, 285A</sup> **B)**, Flag-OsLsi1<sup>d2-40, 276-280A</sup> **C)**, Flag-OsLsi1<sup>d2-40, 282-283A, 285A</sup> **D)**, Flag-OsLsi1<sup>d2-40, L276, 279A</sup> **E)**, Flag-OsLsi1<sup>d2-40, R277, 278, 280A</sup> **F)**, Flag-OsLsi1<sup>d2-40, Q282, 283A</sup> **G)**, and Flag-OsLsi1<sup>d2-40, I285A</sup> **H)** in roots of transgenic lines. Cross-sections of the mature region (15 to 20 mm from the root tip) of the crown roots sampled from transgenic seedlings carrying different variants of *Flag-OsLsi1*<sup>d2-40</sup> were subjected to immunostaining using anti-Flag antibody. Exodermis (Ex) and endodermis (En) in **B) to H)** were enlarged in the left or right of the lower half panel, respectively. Scale bars indicate 50  $\mu$ m in the whole root images or 10  $\mu$ m in the enlarged images. **I)** Polarity index of Flag-OsLsi1 variants at the exodermis and endodermis. Thirty independent root slices from more than 5 independent root slices were used for the quantification of the polarity index. Vertical bars indicate SD. Different letters indicate significant differences at  $P < 0.05$  by Tukey–Kramer’s test.

with Arg at 277, 278, and 280 in N-terminal deleted OsLsi1. The result showed that the substitution of these positively charged residues further decreased the polarity

(Fig. 6, G and H). This further support the importance of a positive charge in generating the polar localization of OsLsi1 at the C-terminus.

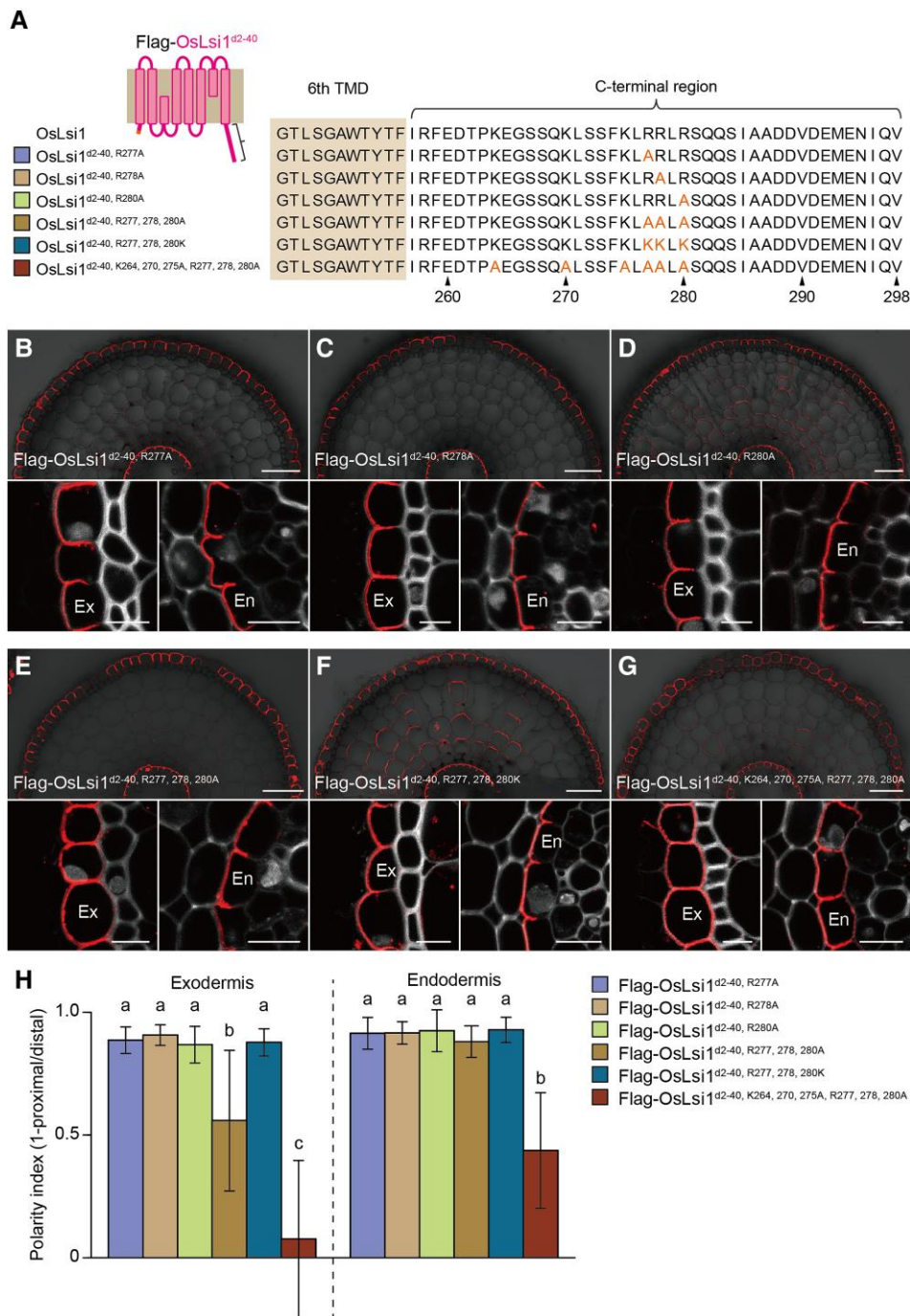


**Figure 6.** Role of positively charged amino acids at the C-terminus of OsLsi1 in the polar localization. **A**) Scheme presentation of substitution sites of positively charged amino acids at the C-terminal region of Flag-OsLsi1<sup>d2-40</sup>. Orange letters show amino acids substituted. **B to G**) Localization of Flag-OsLsi1<sup>d2-40</sup>, R277A **B**), Flag-OsLsi1<sup>d2-40</sup>, R278A **C**), and Flag-OsLsi1<sup>d2-40</sup>, R280A **D**), Flag-OsLsi1<sup>d2-40</sup>, R277, 278, 280A **E**), Flag-OsLsi1<sup>d2-40</sup>, R277, 278, 280K **F**), and Flag-OsLsi1<sup>d2-40</sup>, K264, 270, 275A, R277, 278, 280A **G**) in roots of transgenic lines. Cross-sections of the mature region (15 to 20 mm from the root tip) of the crown roots sampled from transgenic seedlings carrying different variants of Flag-OsLsi1<sup>d2-40</sup> were subjected to immunostaining using anti-Flag antibody. Exodermis (Ex) and endodermis (En) in **B**) to **G**) were enlarged in the left or right of the lower half panel, respectively. Scale bars indicate 50  $\mu$ m in the whole root images or 10  $\mu$ m in the enlarged images. **H**) Polarity index of Flag-OsLsi1 variants at the exodermis and endodermis. Thirty independent cells from more than 5 independent root slices were used for the quantification of the polarity index. Vertical bars indicate sd. Different letters indicate significant differences at  $P < 0.05$  by Tukey–Kramer’s test.

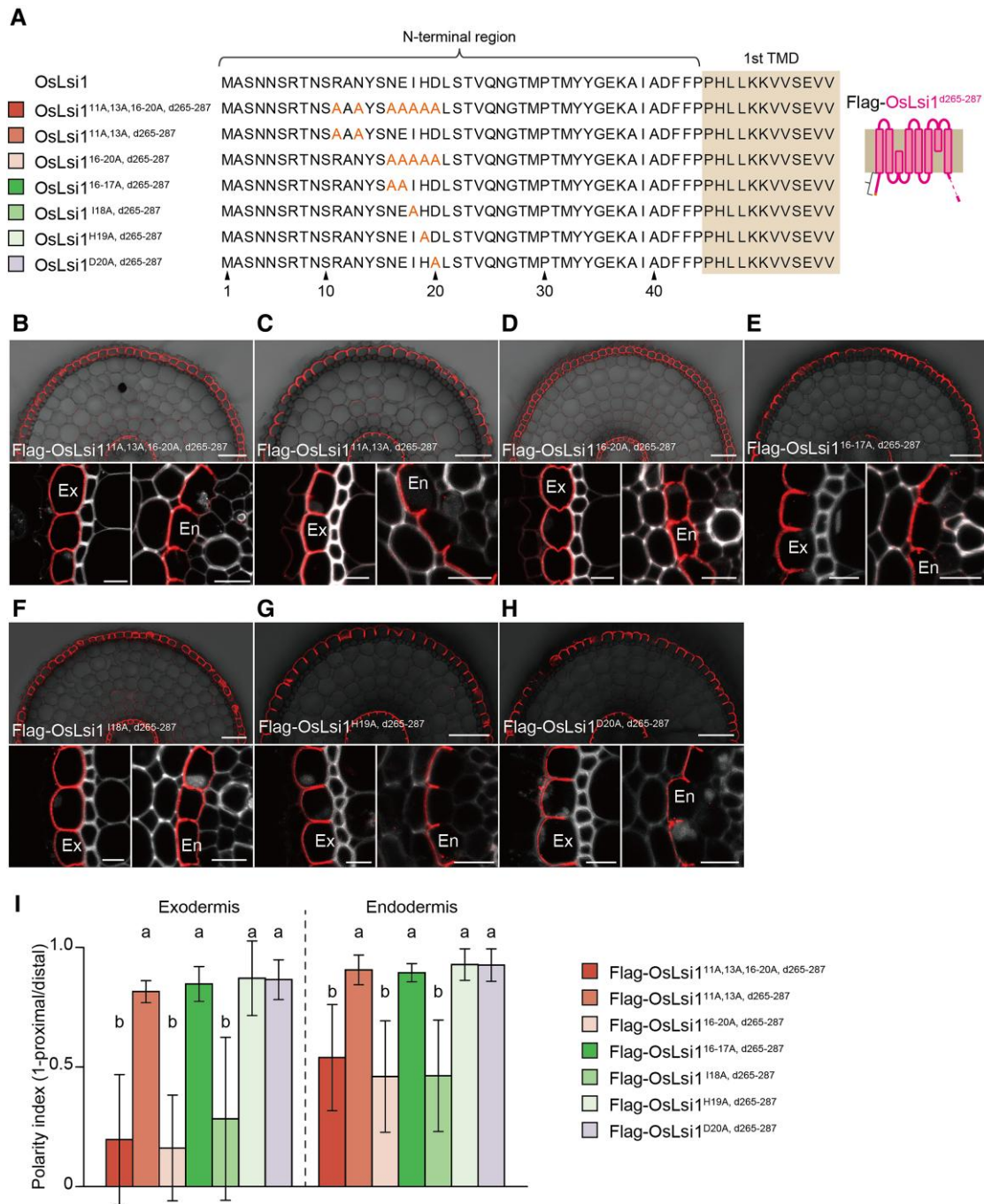


**Figure 7.** Identification of amino acid residues at the N-terminus required for the polar localization. **A**) Scheme presentation of amino acid substitution sites at the N-terminus of Flag-OsLsi1<sup>d265-287</sup>. Orange letters show amino acids substituted. TMD indicates the transmembrane domain. **B–H**) Localization of Flag-OsLsi1<sup>11A, 13A, 16-20A, d265-287</sup> **B**), Flag-OsLsi1<sup>11, 13A, d265-287</sup> **C**), Flag-OsLsi1<sup>16-20A, d265-287</sup> **D**), Flag-OsLsi1<sup>16-17A, d265-287</sup> **E**), Flag-OsLsi1<sup>I18A, d265-287</sup> **F**), Flag-OsLsi1<sup>H19A, d265-287</sup> **G**), and Flag-OsLsi1<sup>D20A, d265-287</sup> **H**) in roots of transgenic lines. Cross-sections of the mature region (15 to 20 mm from the root tip) of the crown roots sampled from transgenic seedlings carrying different variants of *Flag-OsLsi1*<sup>d265-287</sup> were subjected to immunostaining using anti-Flag antibody. Exodermis (Ex) and endodermis (En) in **B**) to **H**) were enlarged in the left or right of the lower half panel, respectively. Scale bars indicate 50  $\mu$ m in the whole root images or 10  $\mu$ m in the enlarged images **B**) to **H**). **I**) Polarity index of Flag-OsLsi1 variants at the exodermis and endodermis. Thirty independent cells from more than 5 independent root slices were used for the quantification of the polarity index. Vertical bars indicate SD. Different letters indicate significant differences at  $P < 0.05$  by Tukey–Kramer’s test.

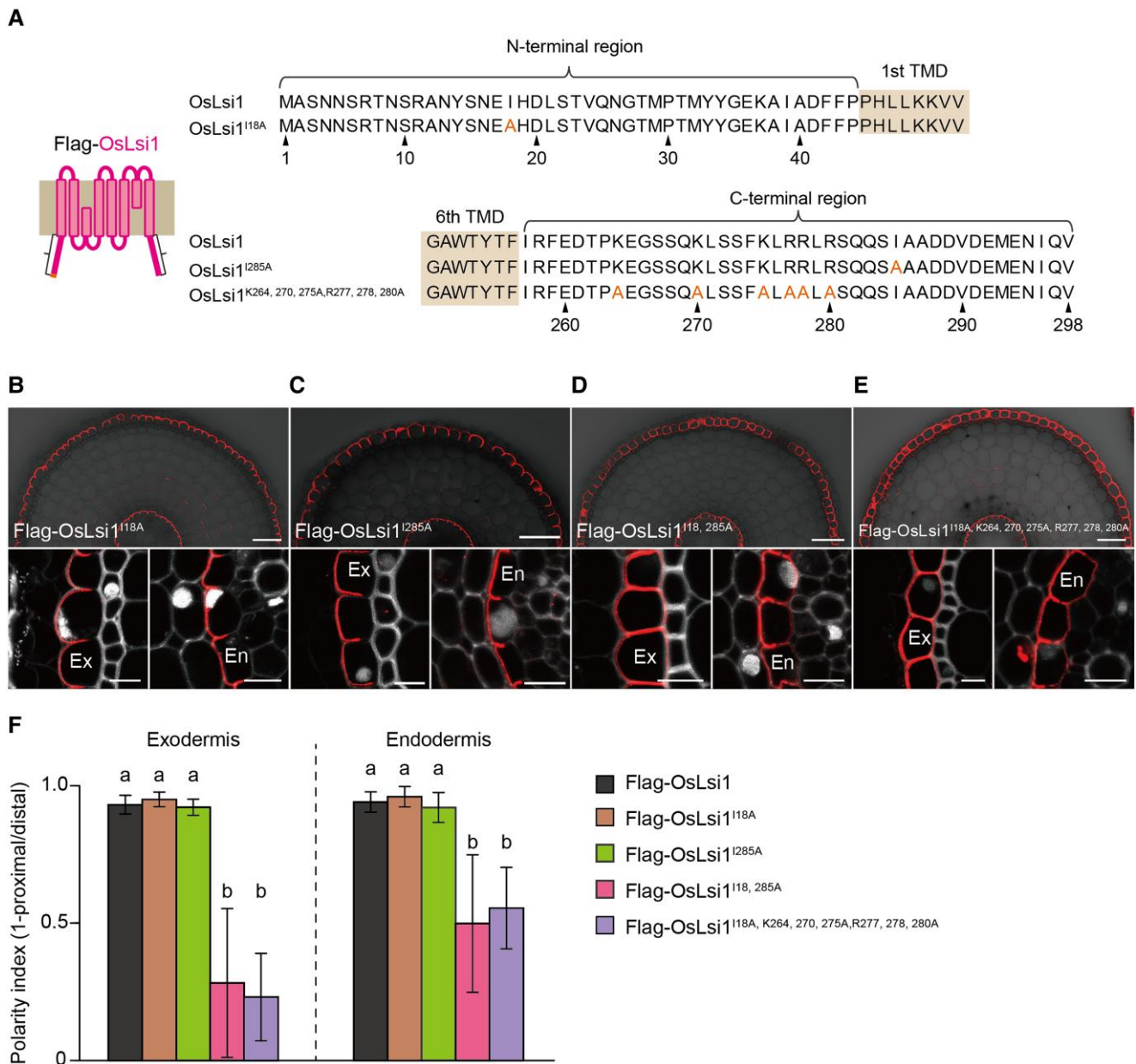


**Figure 8.** Identification of critical amino acids at the C- and N-terminal regions for polar localization of OsLsi1. **A**) Scheme presentation for substitution sites at the N- and C-terminal of full-length OsLsi1. Orange letters show amino acids substituted. TMD indicates the transmembrane domain. **B to E**) Localization of Flag-OsLsi1<sup>I18A</sup> **B**), Flag-OsLsi1<sup>I285A</sup> **C**), Flag-OsLsi1<sup>I18, 285A</sup> **D**), and Flag-OsLsi1<sup>I18A, K264, 270, 275A, R277, 278, 280A</sup> **E**) in roots of transgenic lines. Cross-sections of the mature region (15 to 20 mm from the root tip) of the crown roots sampled from transgenic seedlings carrying different variants of *Flag-OsLsi1* were subjected to immunostaining using anti-Flag antibody. Exodermis (Ex) and endodermis (En) in **B**) to **E**) were enlarged in the left or right of the lower half panel, respectively. Scale bars indicate 50  $\mu$ m in the whole root images or 10  $\mu$ m in the enlarged images **B**) to **E**). **F**) Polarity index of Flag-OsLsi1 variants at the exodermis and endodermis. Thirty independent cells from more than 5 independent root slices were used for the quantification of the polarity index. Vertical bars indicate SD. Different letters indicate significant differences at  $P < 0.05$  by Tukey–Kramer’s test.

### Identification of the amino acid residue at the N-terminus required the polar localization

To identify amino acid residues at the N-terminus critical for the polar localization of OsLsi1, we also performed site-directed mutagenesis using C-terminal deleted OsLsi1 (OsLsi1<sup>d265–287</sup>) (Fig. 7A). Substitutions of amino acid residues at positions 11, 13, and 16 to 20 (OsLsi1<sup>11A, 13A, 16–20A</sup>),

16–20 (OsLsi1<sup>16–20A</sup>), and 18 (OsLsi1<sup>I18A</sup>) only with Ala resulted in a similar reduction of the polarity index at both exodermis and endodermis (Fig. 7, B, D, F, and I). However, substitutions of positions of 11 and 13 (OsLsi1<sup>11A, 13A</sup>), 16 to 17 (OsLsi1<sup>16–17A</sup>), 19 (OsLsi1<sup>H19A</sup>), and 20 (OsLsi1<sup>D20A</sup>) did not affect the polar localization (Fig. 7, C, E, and G–I). Taken together, these findings indicate that Ile18 is a

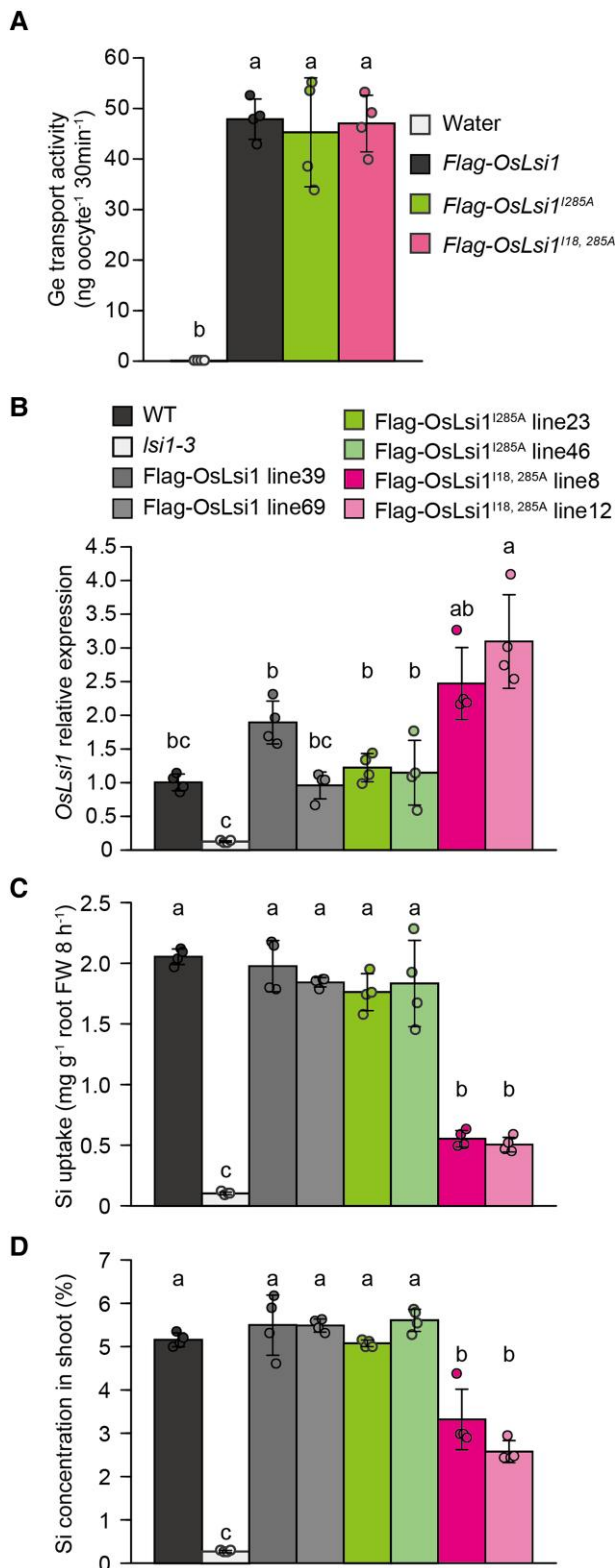


**Figure 9.** Role of OsLsi1 polarity in Si uptake and accumulation in rice. **A**) Transport activity of Flag-OsLsi1 variants for Ge in oocytes. Oocytes expressing Flag-OsLsi1, Flag-OsLsi1<sup>I285A</sup>, or Flag-OsLsi1<sup>I118, 285A</sup> were exposed to MBS with 1 mM GeO<sub>2</sub> for 30 min. The Ge concentration in the oocytes was determined. Data are means ± SD (n = 4). **B to D**) (continued)

crucial residue for the polar localization of OsLsi1 at the N-terminus.

### Confirmation of critical amino acid residues required for the polar localization of OsLsi1

To identify amino acid residues required for the polar localization, we used either N- or C-terminal truncated version of OsLsi1 in the above experiments. To confirm the above results, we further performed site-directed mutagenesis using full-length of OsLsi1 (Fig. 8A). Substitution of either Ile18 at the N-terminus or Ile285 at the C-terminus did not affect the polar localization of OsLsi1 (Fig. 8, B, C, and F). However, when both Ile18 and Ile285 were substituted, the polar localization of OsLsi1 at the exodermis and endodermis was significantly decreased (Fig. 8, D and F), confirming that both the Ile18 and Ile285 are crucial residues for OsLsi1 polar localization. Furthermore, the substitution of Ile18 and 6 positively charged residues at 264, 270, 275, 277, 278, and 280 resulted in decreased polarity index to a similar level of Ile18 and Ile285 substitutions (Fig. 8, E and F). These results indicate that a cluster of positively charged amino acids at the C-terminus also plays an important role in generating polar localization of OsLsi1.

### Significance of polar localization in efficient Si uptake

To investigate the significance of polar localization of OsLsi1 in Si uptake, we compared Si uptake among transgenic rice lines harboring Flag-OsLsi1, Flag-OsLsi1<sup>I285A</sup>, and Flag-OsLsi1<sup>I118, 285A</sup> under the control of OsLsi1 promoter in the *lsi1-3* mutant background. Flag-OsLsi1 and Flag-OsLsi1<sup>I285A</sup> showed polar localization, whereas Flag-OsLsi1<sup>I118, 285A</sup> showed nonpolar localization (Fig. 8). We first compared the transport activity for Ge, an analog of Si, by expressing different OsLsi1 variants in *Xenopus* oocytes. All OsLsi1 variants showed similar transport activity for Ge in oocytes (Fig. 9A), indicating that these substitutions did not affect the transport activity of OsLsi1 variants for Si. The OsLsi1 expression level in the roots was also similar among transgenic lines harboring different OsLsi1 variants, except that the plants carrying Flag-OsLsi1<sup>I118, 285A</sup> showed slightly higher expression than other lines (Fig. 9B). However, the Si uptake (8 h) differed with OsLsi1 variants. The OsLsi1

### Figure 9. (Continued)

Expression levels of OsLsi1 in the roots **B**), short-term Si uptake **C**), and Si accumulation in the shoot **D**) of transgenic plants carrying Flag-OsLsi1, Flag-OsLsi1<sup>I285A</sup> or Flag-OsLsi1<sup>I118, 285A</sup> encoding polar and nonpolar OsLsi1, respectively. For the short-term Si uptake experiment in **C**), transgenic seedlings (22-d-old), as well as wild-type (WT) rice and *lsi1-3* mutant, were exposed to a solution containing 0.5 mM Si for 8 h. At the end of the experiment, the roots were harvested for mRNA extraction and determination of OsLsi1 expression level **B**). For Si accumulation comparison **C**), transgenic seedlings (16-d-old) were exposed to a solution containing 1 mM Si. After 7 d, the shoots were sampled for Si determination. Vertical bars represent the SD of 4 biological replicates. Different letters indicate significant differences at  $P < 0.05$  by Tukey–Kramer's test.

variants showing polar localization, including Flag-OsLsi1 and Flag-OsLsi1<sup>I285A</sup>, completely complemented the Si uptake of the *lsi1-3* mutant, whereas the OsLsi1 variant (Flag-OsLsi1<sup>I18,285A</sup>) having the nonpolar localization only partially complemented the Si uptake which was approximately 30% of the WT (Fig. 9C). Furthermore, we compared Si accumulation in the shoots of different lines after exposure to 1 mM Si for 7 d. As a result, the shoot Si concentration was 40% to 55% lower in transgenic lines having nonpolar OsLsi1 compared with those having polar OsLsi1 (Fig. 9D). These results indicate that polar localization of OsLsi1 plays a crucial role in efficient Si uptake in rice.

## Discussion

Some transporters identified in plants have been reported to show polar localization. For example, it is well known that auxin efflux transporters PIN-FORMED (PIN) show polar localization at the apical and basal sides of a cell, and the mechanisms involved have been well investigated (Naramoto 2017; Marhava 2022; Ramalho et al. 2022). Different from PINs, transporters for mineral nutrients show polar localization at the distal and proximal sides of a cell (Yoshinari and Takano 2017; Che et al. 2018; Huang et al. 2020), but the mechanism underlying the polar localization is poorly understood. In the present study, we identified crucial amino acid residues for polar localization of OsLsi1 in rice, a key transporter for Si uptake (Ma et al. 2006). Furthermore, we showed experimental evidence for the significance of the transporter polarity in efficient Si uptake.

### Amino acid residues required for trafficking and polar localization of OsLsi1

By taking advantage of immunostaining and transgenic lines harboring various variants of Flag-OsLsi1, we were able to identify amino acid residues required for trafficking and the polar localization of OsLsi1. Trafficking of OsLsi1 from ER to the plasma membrane is only controlled by one region from 288 to 298 at the C-terminus (Supplemental Figs. S3 and S4). This region might be involved in quality control or recognition by the COPII-mediated membrane trafficking system in the ER (Marti et al. 2010; Strasser 2018).

On the other hand, the polar localization of OsLsi1 requires different regions at both N- and C-termini (Supplemental Fig. S1, S2, and S4). Further analysis with site-directed mutagenesis revealed 2 critical amino acid residues for the polar localization; Ile18 at the N-terminus and Ile285 at the C-terminus (Figs. 5 and 7). This is supported by the finding that substitution of both Ile18 and Ile285 resulted in the loss of the polar localization of OsLsi1, although a single substitution of either residue still maintained the polar localization (Fig. 8). The exact role of these 2 residues in polar localization remains to be investigated in the future, but one possibility is that they are involved in polar exocytosis, which is proposed to be one of mechanism for the polar localization (Kleine-Vehn et al. 2011;

Langowski et al. 2016). For example, knockout of *EXOCYST84b* (*AtEXO84b*), one of the components of the exocyst complex, a tethering complex mediating the initial encounter of arriving exocytic vesicles at the plasma membrane, impaired the polar localization of PENETRATION3 (PEN3), an ATP-binding cassette transporter involved in defense against some fungal pathogens (Mao et al. 2016). However, it remains to be investigated whether exocyst complex is required for the polar localization of OsLsi1.

### Conservation of crucial amino acid residues for polar localization of OsLsi1 in different plant species

Several orthologs of OsLsi1 have been identified in other plant species. Some orthologs, such as HvLsi1, ZmLsi1, and CsLsi1, show polar localization like OsLsi1, whereas others, such as CmLsi1 and SLsi1, show nonpolar localization (Chiba et al. 2009; Mitani et al. 2009, 2011; Sun et al. 2017, 2020). By comparing the residues identified in the present study, Ile18 was conserved in HvLsi1 and ZmLsi1 but not in CsLsi1, CmLsi1, and SLsi1 (Supplemental Fig. S7). Ile285 was only observed in OsLsi1 but not in others (Supplemental Fig. S7). These observations suggest that the Ile18-mediated polarity system is conserved in Poaceae, whereas the Ile285-mediated system only occurs in rice. In contrast, part of positively charged residues, including Lys275, Arg277, and Arg278, are conserved in all Lsi1 orthologs (Supplemental Fig. S7). Furthermore, some other positively charged residues at the flanking position of Lys264, Lys270, and Arg280 of OsLsi1 are also conserved in all orthologs (Supplemental Fig. S7). The polar localization of CsLsi1 might be generated through these positively charged residues. In contrast, pumpkin and tomato might not have the polarity regulation system, although some positively charged residues are conserved in CmLsi1 and SLsi1. In fact, CmLsi1 shows polar localization when it is ectopically expressed in rice roots (Mitani et al. 2011). Further studies are required for mechanisms of polar localization in Lsi1 orthologues in different plant species.

On the other hand, there are 9 aquaporins belonging to the NIP subgroup in the rice genome (Sakurai et al. 2005). Among them, OsLsi1, OsLsi6 for Si transport, and OsNIP3;1 for B transport show polar localization, whereas OsNIP1;1 and OsNIP3;3 show nonpolar localization (Ma et al. 2006; Yamaji et al. 2008; Shao et al. 2018; Sun et al. 2018). Comparison of sequences indicated that Ile18 and some positively charged residues, such as Lys270, Lys275, Arg277, and Arg278, but not Ile285, were conserved in OsLsi6 (Supplemental Fig. S8). In contrast, there were no such residues in OsNIP1;1 and OsNIP3;3 (Supplemental Fig. S8). This difference is most likely the reason for the polar or nonpolar localization of these proteins, which is also supported by the finding that OsNIP1;1 fused with OsLsi1 C-terminus showed polar localization (Fig. 2). On the other hand, OsNIP3;1 does not have any residues identified in OsLsi1 (Supplemental Fig. S8). Instead of these residues, OsNIP3;1 has TPG repeat at the N-terminus, which is another polarity regulation motif identified from AtNIP5;1, an ortholog of OsNIP3;1 in

Arabidopsis (Wang et al. 2017). This TPG repeat-mediated system might regulate the polar localization of OsNIP3;1 independent of residues identified in OsLsi1.

### Distinct mechanism underlying polar localization of OsLsi1 in rice

Endocytosis has been reported to be involved in the maintenance of the polar localization of mineral transporters such as AtNIP5;1 and AtBOR1 in Arabidopsis (Wang et al. 2017; Yoshinari et al. 2019). The polarity is maintained by the phosphorylation of TPG repeat at the N-terminus through regulation of AP2-dependent constitutive CME in AtNIP5;1 (Wang et al. 2017). AP2-dependent constitutive CME is also required to maintain the polarity of AtBOR1 (Yoshinari et al. 2019). The latter half of the C-terminal cytosolic tail (Arg637–Asn704) of AtBOR1 is recognized by the  $\mu$  subunit of the AP2 complex (Yoshinari et al. 2019). Furthermore, 3 tyrosine-based signal motifs, Yxx $\Phi$  (Y; tyrosine, x; any amino acid,  $\Phi$ ; any bulky hydrophobic residue), are also involved in the maintenance of the polar localization of AtBOR1 in the cytosolic loop region (Takano et al. 2010). However, we found that AP2-dependent CME (Konishi et al. 2022), phosphorylation, and tyrosine-based signal motif are not required for the polar localization of OsLsi1 (Figs. 4 and 8), suggesting a distinct mechanism underlying the polar localization of OsLsi1 in rice.

Yxx $\Phi$  motifs in AtBOR1 are required for the interaction with AP3 and AP4 complexes (Yoshinari et al. 2019), suggesting potential regulation systems for its polar localization through AP3- and AP4-dependent pathways. Although AP3 and AP4 are generally involved in the protein sorting to the vacuole (Shimizu and Uemura 2022), these adaptor proteins might be potential candidates for a regulator of the polar localization of OsLsi1, which needs to be examined in the future.

Furthermore, ubiquitination of Lys residues has been reported in polar mineral transporters such as AtIRT1 and AtBOR1 (Barberon et al. 2011; Kasai et al. 2011; Yoshinari et al. 2021). The monoubiquitination of Lys154 and Lys179 is required for the constitutive internalization of AtIRT1 from the plasma membrane to the early endosome (Barberon et al. 2011), and polyubiquitination of these Lys residues is necessary for degradation from the early endosome to the vacuole under excess metal conditions (Dubeaux et al. 2018). Polyubiquitination of Lys590 is also necessary for high B-induced degradation of AtBOR1 (Kasai et al. 2011; Yoshinari et al. 2021). However, the Lys mutations at the C-terminus of OsLsi1 did not affect the polar localization (Fig. 4), suggesting that the Lys modifications are not necessary for the polarity regulations of OsLsi1.

### Mechanisms involved in polar localization of OsLsi1 may partially differ at the exodermis and endodermis

OsLsi1 is polarly localized at both the exodermis and endodermis (Ma et al. 2006). Our results suggest that the mechanisms underlying OsLsi1 polarity somewhat differ between the exodermis and endodermis. Although Ile18 and Ile285 are

important for the polar localization of OsLsi1 at both the exodermis and endodermis (Fig. 8), 3 positively charged amino acids have a different effect on the polar localization of OsLsi1 at the exodermis and endodermis. Substitution of Arg277, Arg278, and Arg280 by Ala significantly reduced the polar localization of OsLsi1 at the exodermis, but had less or no effect on the polar localization of OsLsi1 at the endodermis (Figs. 5 and 6). This difference could be attributed to the different features of CS at the exodermis and endodermis in rice. Different from Arabidopsis, rice roots have 2 CS at the exodermis and endodermis, where OsLsi1 is localized (Ma et al. 2006). Suberin deposition is required for CS formation at the exodermis (Shiono et al. 2014), whereas lignin accumulation is necessary for that of the endodermis (Wang et al. 2019). CS localized at the root endodermis has been reported to play an additional role in polarity maintenance through the limitation of lateral diffusion of mineral transporters in Arabidopsis (Alassimone et al. 2010; Yoshinari et al. 2019). For example, AtNIP5;1 and AtBOR1 were fully divided by CS in the developed endodermis (Alassimone et al. 2010). Similarly, OsLsi1 at the endodermis is also clearly separated by CS (Konishi et al. 2022). However, at the exodermis, part of OsLsi1 is over-crossed the CS (Konishi et al. 2022). This observation suggests that different from CS at the endodermis, the CS at the exodermis is not involved in maintaining the lateral polarity by blocking the lateral diffusion of transporters (Konishi et al. 2022).

Since the substitution of Arg277, Arg278, and Arg280 by positively charged amino acid, Lys, did not affect the polar localization of OsLsi1 at the exodermis (Fig. 6), it seems that electrostatic interaction with negatively charged compounds might be involved in this regulation. Acidic phospholipids are candidates for interaction with these positively charged residues because some acidic phospholipids are necessary for the polar localization of the plasma membrane proteins. For example, the phosphatidylinositol 4 phosphate and phosphatidylinositol 4, 5 bisphosphates showed polar localization in the epidermis cell of Arabidopsis root (Tejos et al. 2014), and the interaction between polarly localized phosphatidylinositol 4, 5 bisphosphates is required for donut-like polar localization of PIN complex in protophloem sieve elements (Marhava et al. 2020). Furthermore, the electrostatic interaction between phosphatidic acid and EXO70A is crucial for the polar localization of the exocyst complex (Synek et al. 2021). It will be interesting to investigate whether these compounds are also involved in the polar localization of OsLsi1 in the future.

### Significance of OsLsi1 polarity in efficient Si uptake

In rice, high Si uptake is achieved by a pair of Si transporters, OsLsi1 and OsLsi2 (Ma and Yamaji 2015). OsLsi2 is a proton-dependent efflux transporter for silicic acid, which is also expressed at the exodermis and endodermis, but localized at the proximal side (Ma et al. 2007). Therefore, OsLsi1 and OsLsi2 form an efficient pathway for Si uptake; Si in soil solution is first imported into the exodermis by OsLsi1 and exported by OsLsi2 to the aerenchyma, followed by

importing Si by OsLsi1 into the endodermis cells and exporting to the stele by OsLsi2 (Ma and Yamaji 2015).

A previous study with mathematical modeling simulated that the polar localization of OsLsi1 is crucial for efficient Si uptake in rice (Sakurai et al. 2015). In the present study, we showed experimental evidence on the significance of the polar localization of OsLsi1 in Si uptake by taking advantage of transgenic plants with and without the polarity of OsLsi1. The transgenic plants with nonpolar localization of OsLsi1 showed significantly lower Si uptake and accumulation compared with those with polar localization (Fig. 9). Since the expression level and transport activity were comparable between polar and nonpolar OsLsi1 (Fig. 9), this significant decrease is mainly attributed to the loss of polar localization of OsLsi1. OsLsi1 is a bidirectional channel that mediates concentration-dependent passive transport of Si; therefore, its polar localization cooperated with OsLsi2 is important for forming an efficient directional transport system for Si uptake (Fig. 9). The importance of transporter polarity for efficient uptake of some mineral elements was also reported in Arabidopsis. For example, loss of polarity of AtNIP5;1 and AtBOR1 decreased B uptake in Arabidopsis (Wang et al. 2017; Yoshinari et al. 2019). Nonpolar localization of AtIRT1 reduced metal accumulations under Fe deficiency (Barberon et al. 2014).

In conclusion, we identified amino acid residues required for trafficking and polar localization of OsLsi1 in rice. We also found that phosphorylation and Lys modifications are not involved in the polar localization of OsLsi1, representing a distinct mechanism for polar localization of B transporters in Arabidopsis. Furthermore, we provided experimental evidence for the importance of transporter polarity in efficient nutrient uptake.

## Materials and methods

### Plant materials and growth conditions

The wild-type rice (WT, *O. sativa*, cv. Nipponbare) and various transgenic lines generated as described below were used in this study. The seeds were soaked in water for 2 d in the dark at 30 °C, and then transferred on a net floating in a 0.5 mM CaCl<sub>2</sub> solution. Seedlings were then transferred to the half-strength Kimura B solution (pH 5.6), which contained the macronutrients (mM); 0.18 (NH<sub>4</sub>)<sub>2</sub>SO<sub>4</sub>, 0.27 MgSO<sub>4</sub>·7H<sub>2</sub>O, 0.09 KNO<sub>3</sub>, 0.18 Ca(NO<sub>3</sub>)<sub>2</sub>·4H<sub>2</sub>O, and 0.09 KH<sub>2</sub>PO<sub>4</sub>, and the micronutrients (μM); 2 FeSO<sub>4</sub>, 3 H<sub>3</sub>BO<sub>3</sub>, 1 (NH<sub>4</sub>)<sub>6</sub>Mo<sub>7</sub>O<sub>24</sub>, 0.5 MnCl<sub>2</sub>, 0.4 ZnSO<sub>4</sub>, and 0.2 CuSO<sub>4</sub>. The pH of the solution was adjusted to 5.6 by 1N NaOH. The nutrient solution was renewed every 2 d. Plants were grown in a greenhouse at 25 to 30 °C under natural light. Replicates are indicated in each figure legend.

### Generation of transgenic lines harboring various variants of *Flag-OsLsi1* and *Flag-OsNIP1;1*

Coding sequence (CDS) of *OsNIP1;1* was first amplified from rice root cDNA by PCR, and *Flag-tag* was fused at the

N-terminal by overlapping PCR. To generate *Flag*-tagged *OsLsi1* deletion constructs, site-directed mutagenesis was performed by overlapping PCR. To construct chimera between *OsNIP1;1* and *OsLsi1*, the various *OsLsi1* CDS regions were fused to N- or C-terminal deleted *OsNIP1;1* CDS by overlapping PCR. Plasmids of *Flag-OsNIP1;1*, or *Flag-OsLsi1*, as described previously (Huang et al. 2022), were used as a template for these PCR reactions. To generate N- or C-terminal substitution variants of *OsLsi1*, site-directed mutagenesis was performed by overlapping PCR. *Flag-OsLsi1*<sup>d2–40</sup> or *Flag-OsLsi1*<sup>d265–287</sup> was used as a template for these PCR reactions. The resultant PCR products were cloned into a *pTA2* cloning vector (Toyobo). Variants of *Flag-OsLsi1* and *Flag-OsNIP1;1* were subcloned behind the *OsLsi1* promoter (2,000 bp) of *pZP2H-lac* vector as described previously (Huang et al. 2022) using *HindIII* and *XbaI* restriction sites. *Nopaline synthase* gene terminator was inserted behind the CDS of variants using *SacI* restriction site of *pZP2H-lac* vector. Each construct was transformed into calluses of *OsLsi1* loss-of-function mutant (Chiba et al. 2009; *lsi1-3*) by *Agrobacterium tumefaciens* mediated transformation (Hiei et al. 1994). All primers and templates used in the above PCR experiments are listed in Supplemental Data Set 1.

### Immunostaining analysis

To observe tissue and subcellular localization of *OsLsi1* and *OsNIP1;1* variants generated above, root samples were taken from the transgenic seedlings 6th to 7th leaf stage at T0 or T1 generation. T1 generation of seeds was soaked in water at 30 °C in the dark for 2 d and then transferred to a net floating on a 0.5 mM CaCl<sub>2</sub> solution. On Day 4, the seedlings (T1 generation or after regeneration at T0 generation) were hydroponically cultivated in a half-strength Kimura B solution as described above. Immunostaining was performed according to Ma et al. (2006) and Konishi and Ma (2021). After the fixation, cross-sections of mature crown root (15 to 20 mm from the tip) and lateral root were prepared by MicroSlicer (LinearSlicer PRO10, Dosaka EM, Co., Ltd). For detection of the *Flag* signal, a rat monoclonal *Flag* (DYKDDDDK) epitope tag antibody (L5, 1/1,000, Novus Biologicals) was used as a primary antibody. In some experiments, double immunostaining with antibodies against *Flag* and marker proteins, including rabbit polyclonal antibody of *OsNramp5* (Sasaki et al. 2012; 1/2,000), *OsBOR1* (Shao et al. 2021; 1/2,000), and monoclonal antibody of HDEL (2E7, 1/500, Santa Cruz Biotechnology, Inc.), were used as a primary antibody, respectively. The primary antibody was labeled by Alexa Fluor 488 goat antirat IgG (Thermo Fisher Scientific) for *Flag-tag*, Alexa Fluor 555 goat antirabbit IgG (Thermo Fisher Scientific) for *OsNramp5* and *OsBOR1*, and Alexa Fluor 555 goat antimouse IgG (Thermo Fisher Scientific) for HDEL, respectively. After incubation with a secondary antibody, the nucleus was stained by 4',6-diamidino-2-phenylindole (DAPI). Signals were observed with a confocal laser scanning microscope (TCS SP8X, Leica). HC PL APO CS2 x20/0.75 air objective lens or HC PL APO CS2 x63/1.4 oil immersion objective lens was used for the whole root or enlarged



image observation, respectively. Alexa Fluor 488 or Alexa Fluor 555 was excited by a 488 nm or a 555 nm laser, and their emission was collected at 510 to 525 nm or 563 to 580 nm, respectively. The laser intensity was modulated depending on the staining levels, while the gain was set to 100%.

The signal intensity was quantified using the line quantification tool of LAS AF Lite software ver 4.0 (Leica Microsystems). Thirty cells from more than 5 independent slices were used for quantification. The polarity index was calculated from the ratio of signal intensity between the distal and proximal sides in each cell of exodermis or endodermis, respectively (Supplemental Fig. S6). Magnified images were taken for high-resolution images in Supplemental Figs. S1 and S2, and deconvolution was applied using the Huygens Essentials software (Scientific Volume Imaging B.V.).

### Si uptake and accumulation determination

Seedlings (22-d-old) of wild-type (WT), *lsl1-3* mutant, 2 independent transgenic plants carrying *Flag-OsLsi1*, *Flag-OsLsi1<sup>I285A</sup>*, or *Flag-OsLsi1<sup>I18, 285A</sup>*, were used for Si uptake experiments. The seedlings were prepared as described above. The uptake solution contained 0.5 mM Si as silicic acid in a 50 mL black bottle. Silicic acid was prepared by passing potassium silicate through cation-exchange resin (Amberlite IR-120B, H<sup>+</sup> form, Organo, Tokyo; Ma et al. 2002). After 8 h, a 0.5 mL aliquot of uptake solution was taken for the determination of Si concentration by the colorimetric molybdenum blue method (Ma et al. 2003). Transpiration (water loss) was recorded at the end of the experiment. Roots were harvested and stored in liquid nitrogen for RNA extraction after recording root fresh weight. Four biological replicates were used for this experiment.

To compare Si accumulation in the shoots, seedlings (16-d-old) of the above lines were grown in a half-strength Kimura B solution containing 1 mM Si. The solution was changed every 2 d. After 7 d, the shoot parts were harvested and dried in a 70 °C oven for 3 d. After recording the shoot dry weight, each sample was digested in a mixture of 4 mL of HNO<sub>3</sub> (62%), 4 mL of H<sub>2</sub>O<sub>2</sub> (30%), and 1 mL of hydrofluoric acid (46%) in a microwave (Microwave Digestion System START D, Millstone Co., Ltd.). The digested solution was diluted to 50 mL with 4% (w/v) boric acid. The Si concentration in the digest solution was determined by the colorimetric molybdenum blue method. Four biological replicates were made for this experiment.

### Ge transport assay in oocyte

Oocytes for transport activity assay were isolated from *Xenopus laevis*. Procedures for deflocculation, culture conditions, and selection were the same as described previously (Ma et al. 2006). CDS of *OsLsi1* variants, including *Flag-OsLsi1*, *Flag-OsLsi1<sup>I285A</sup>*, and *Flag-OsLsi1<sup>I18, 285A</sup>*, were amplified from plasmids generated above by PCR. These CDSs were inserted into the *Bgl*III site of a *Xenopus* oocyte expression vector, *pXβG-ev1*. Capped RNA was synthesized by in vitro transcription with a mMESSAGE mMACHINE High Yield

Capped RNA Transcription Kit (Thermo Fisher Scientific). A volume of 50 nL (1 ng nL<sup>-1</sup>) cRNA or RNase-free water as a negative control was injected into the oocyte. After 1 d of incubation in Modified Barth's Saline (MBS) at 18 °C, oocytes were exposed to MBS with 1 mM GeO<sub>2</sub> for 30 min at 18 °C. At the end of the uptake, the oocytes were washed in ice-cold MBS and digested with HNO<sub>3</sub>. Ge concentration in the digested solution was determined by inductively coupled plasma-mass spectrometry (7700X; Agilent Technologies). Four biological replicates were made for this experiment.

### RNA extraction and quantitative Rt-PCR analysis

To investigate the expression level of *OsLsi1* variants in transgenic lines, root samples were harvested with 4 replicates at the end of the Si uptake experiment as described above (see the section "Si uptake and accumulation determination"). Total RNA was extracted by RNeasy PlantMini kit (Qiagen) following the manufacturer's instruction. The cDNA was synthesized by ReverTra Ace qPCR RT Master Mix with gDNA Remover (Toyobo). The gene expression level of *OsLsi1* was determined using the KOD SYBR qPCR mix (Toyobo) on a CFX384 system (Bio-Rad) using the specific primers described previously (Ma et al. 2006). *Histone H3* was used as an internal control (Mitani et al. 2011). The relative expression level was calculated using the comparative C<sub>t</sub> method.

### Statistical analysis

ANOVA, followed by Tukey–Kramer's test, was used for comparison using the software BellCurve for Excel (Social Survey Research Information Co., Ltd). Statistical data are provided in Supplemental Data Set 2.

### Accession numbers

The RAP-DB accession numbers for the genes examined in this study are as follows: *OsLsi1* (Os02g0745100), *OsNIP1;1* (Os02g0232900).

### Supplemental data

The following materials are available in the online version of this article.

**Supplemental Figure S1.** Subcellular localization of *Flag-OsLsi1<sup>d265–298</sup>* in rice roots.

**Supplemental Figure S2.** Subcellular localization of *Flag-OsLsi1<sup>d2–40, d265–298</sup>* in rice roots.

**Supplemental Figure S3.** Identification of region for membrane trafficking of *OsLsi1* in the C-terminal region.

**Supplemental Figure S4.** The localization of the deletion variant of *Flag-OsLsi1<sup>d265–287</sup>*.

**Supplemental Figure S5.** Localization of chimera protein between *OsNIP1;1* and *OsLsi1* in rice roots.

**Supplemental Figure S6.** Quantification of the polarity index.

**Supplemental Figure S7.** Sequence comparison between polar and nonpolar *Lsi1* orthologs.

**Supplemental Figure S8.** Sequence comparison between polar and nonpolar NIP-type aquaporins in rice.

**Supplemental Data Set 1.** Primer sequences and templates for the construction of various variants of *OsLsi1* and *OsNIP1;1*.

**Supplemental Data Set 2.** Statistical data.

## Funding

This work was supported by Japan Society for the Promotion of Science (JSPS KAKENHI Grant Numbers 16H06296 and 21H05034 to J.F.M.).

## Author contributions

N.K., N.Y., and J.F.M. conceived and designed the experiments; N.K. and N.M.U. performed experiments. N.K. and J.F.M. analyzed data and wrote the manuscript.

*Conflict of interest statement.* All authors state no conflict of interest concerning this paper.

## References

- Alassimone J, Naseer S, Geldner N.** A developmental framework for endodermal differentiation and polarity. *Proc Natl Acad Sci USA*. 2010;**107**(11):5214–5219. <https://doi.org/10.1073/pnas.0910772107>
- Barberon M, Dubeaux G, Kolb C, Isono E, Zelazny E, Vert G.** Polarization of IRON-REGULATED TRANSPORTER 1 (IRT1) to the plant-soil interface plays crucial role in metal homeostasis. *Proc Natl Acad Sci USA*. 2014;**111**(22):8293–8298. <https://doi.org/10.1073/pnas.1402262111>
- Barberon M, Geldner N.** Radial transport of nutrients: the plant root as a polarized epithelium. *Plant Physiol*. 2014;**166**(2):528–537. <https://doi.org/10.1104/pp.114.246124>
- Barberon M, Zelazny E, Robert S, Conéjéro G, Curie C, Friml J, Vert G.** Monoubiquitin-dependent endocytosis of the iron-regulated transporter 1 (IRT1) transporter controls iron uptake in plants. *Proc Natl Acad Sci USA*. 2011;**108**(32):E450–E458. <https://doi.org/10.1073/pnas.1100659108>
- Che J, Yamaji N, Ma JF.** Efficient and flexible uptake system for mineral elements in plants. *New Phytol*. 2018;**219**(2):513–517. <https://doi.org/10.1111/nph.15140>
- Chiba Y, Mitani N, Yamaji N, Ma JF.** Hvlsi1 is a silicon influx transporter in barley. *Plant J*. 2009;**57**(5):810–818. <https://doi.org/10.1111/j.1365-3113X.2008.03728.x>
- Dubeaux G, Neveu J, Zelazny E, Vert G.** Metal sensing by the IRT1 transporter-receptor orchestrates its own degradation and plant metal nutrition. *Mol Cell*. 2018;**69**(6):953–964. <https://doi.org/10.1016/j.molcel.2018.02.009>
- Enstone DE, Peterson CA, Ma F.** Root endodermis and exodermis: structure, function, and responses to the environment. *J Plant Growth Regul*. 2002;**21**(4):335–351. <https://doi.org/10.1007/s00344-003-0002-2>
- Gordon-Weeks R, Tong Y, Davies TE, Leggewie G.** Restricted spatial expression of a high-affinity phosphate transporter in potato roots. *J Cell Sci*. 2003;**116**(15):3135–3144. <https://doi.org/10.1242/jcs.00615>
- Guo Z, Cao H, Zhao J, Bai S, Peng W, Li J, Sun L, Chen L, Lin Z, Shi C, et al.** A natural uORF variant confers phosphorus acquisition diversity in soybean. *Nat Commun*. 2022;**13**(1):1–14. <https://doi.org/10.1038/s41467-022-31555-2>
- Hiei Y, Ohta S, Komari T, Kumashiro T.** Efficient transformation of rice (*Oryza sativa* L.) mediated by *Agrobacterium* and sequence analysis of the boundaries of the T-DNA. *Plant J*. 1994;**6**(2):271–282. <https://doi.org/10.1046/j.1365-3113X.1994.6020271.x>
- Huang S, Konishi N, Yamaji N, Shao JF, Mitani-Ueno N, Ma JF.** Boron uptake in rice is regulated post-translationally via a clathrin-independent pathway. *Plant Physiol*. 2022;**188**(3):1649–1664. <https://doi.org/10.1093/plphys/kiab575>
- Huang S, Wang P, Yamaji N, Ma JF.** Plant nutrition for human nutrition: hints from rice research and future perspectives. *Mol Plant*. 2020;**13**(6):825–835. <https://doi.org/10.1016/j.molp.2020.05.007>
- Kasai K, Takano J, Miwa K, Toyoda A, Fujiwara T.** High boron-induced ubiquitination regulates vacuolar sorting of the BOR1 borate transporter in *Arabidopsis thaliana*. *J Biol Chem*. 2011;**286**(8):6175–6183. <https://doi.org/10.1074/jbc.M110.184929>
- Kiba T, Feria-Bourrellier AB, Lafouge F, Lezhneva L, Boutet-Mercery S, Orsel M, Bréhaut V, Miller A, Daniel-Vedele F, Sakakibara H, et al.** The *Arabidopsis* nitrate transporter NRT2.4 plays a double role in roots and shoots of nitrogen-starved plants. *Plant Cell*. 2012;**24**(1):245–258. <https://doi.org/10.1105/tpc.111.092221>
- Kleine-Vehn J, Wabnik K, Martiniere ŁŁ, Willig K, Naramoto S, Leitner J, Tanaka H, Jakobs S, Robert S, Luschig C, et al.** Recycling, clustering, and endocytosis jointly maintain PIN auxin carrier polarity at the plasma membrane. *Mol Syst Biol*. 2011;**7**(1):540. <https://doi.org/10.1038/msb.2011.72>
- Konishi N, Huang S, Yamaji N, Ma JF.** Cell-type-dependent but CME-independent polar localization of silicon transporters in rice. *Plant Cell Physiol*. 2022;**63**(5):699–712. <https://doi.org/10.1093/pcp/pcac032>
- Konishi N, Ma JF.** Three polarly localized ammonium transporter 1 members are cooperatively responsible for ammonium uptake in rice under low ammonium condition. *New Phytol*. 2021;**232**(4):1778–1792. <https://doi.org/10.1111/nph.17679>
- Łangowski Ł, Wabnik K, Li H, Vanneste S, Naramoto S, Tanaka H, Friml J.** Cellular mechanisms for cargo delivery and polarity maintenance at different polar domains in plant cells. *Cell Discov*. 2016;**2**(1):1–18. <https://doi.org/10.1038/celldisc.2016.18>
- Ma JF, Higashitani A, Sato K, Takeda K.** Genotypic variation in silicon concentration of barley grain. *Plant Soil*. 2003;**249**(2):383–387. <https://doi.org/10.1023/A:1022842421926>
- Ma JF, Tamai K, Ichii M, Wu GF.** A rice mutant defective in Si uptake. *Plant Physiol*. 2002;**130**(4):2111–2117. <https://doi.org/10.1104/pp.010348>
- Ma JF, Tamai K, Yamaji N, Mitani N, Konishi S, Katsuhara M, Ishiguro M, Murata Y, Yano M.** A silicon transporter in rice. *Nature*. 2006;**440**(7084):688–691. <https://doi.org/10.1038/nature04590>
- Ma JF, Yamaji N.** A cooperative system of silicon transport in plants. *Trends Plant Sci*. 2015;**20**(7):435–442. <https://doi.org/10.1016/j.tplants.2015.04.007>
- Ma JF, Yamaji N, Mitani N, Tamai K, Konishi S, Fujiwara T, Katsuhara M, Yano M.** An efflux transporter of silicon in rice. *Nature*. 2007;**448**(7150):209–212. <https://doi.org/10.1038/nature05964>
- Ma JF, Yamaji N, Mitani N, Xu XY, Su YH, McGrath SP, Zhao FJ.** Transporters of arsenite in rice and their role in arsenic accumulation in rice grain. *Proc Natl Acad Sci USA*. 2008;**105**(29):9931–9935. <https://doi.org/10.1073/pnas.0802361105>
- Mao H, Nakamura M, Viotti C, Grebe M.** A framework for lateral membrane trafficking and polar tethering of the PEN3 ATP-binding cassette transporter. *Plant Physiol*. 2016;**172**(4):2245–2260. <https://doi.org/10.1104/pp.16.01252>
- Marhava P.** Recent developments in the understanding of PIN polarity. *New Phytol*. 2022;**233**(2):624–630. <https://doi.org/10.1111/nph.17867>
- Marhava P, Fandino ACA, Koh SW, Jelínková A, Kolb M, Janacek DP, Breda AS, Cattaneo P, Hammes UZ, Petrášek J, et al.** Plasma membrane domain patterning and self-reinforcing polarity in *Arabidopsis*. *Dev Cell*. 2020;**52**(2):223–235. <https://doi.org/10.1016/j.devcel.2019.11.015>
- Marti L, Fornaciari S, Renna L, Stefano G, Brandizzi F.** COPII-mediated traffic in plants. *Trends Plant Sci*. 2010;**15**(9):522–528. <https://doi.org/10.1016/j.tplants.2010.05.010>

- Millar AH, Heazlewood JL, Gligione C, Holdsworth MJ, Bachmair A, Schulze WX.** The scope, functions, and dynamics of posttranslational protein modifications. *Annu Rev Plant Biol.* 2019;**70**(1):119–151. <https://doi.org/10.1146/annurev-arplant-050718-100211>
- Mitani-Ueno N, Yamaji N, Zhao FJ, Ma JF.** The aromatic/arginine selectivity filter of NIP aquaporins plays a critical role in substrate selectivity for silicon, boron, and arsenic. *J Exp Bot.* 2011;**62**(12):4391–4398. <https://doi.org/10.1093/jxb/err158>
- Mitani N, Yamaji N, Ago Y, Iwasaki K, Ma JF.** Isolation and functional characterization of an influx silicon transporter in two pumpkin cultivars contrasting in silicon accumulation. *Plant J.* 2011;**66**(2):231–240. <https://doi.org/10.1111/j.1365-3113X.2011.04848.x>
- Mitani N, Yamaji N, Ma JF.** Characterization of substrate specificity of a rice silicon transporter, *Lsi1*. *Pflüg Arch Eur J Physiol.* 2008;**456**(4):679–686. <https://doi.org/10.1007/s00424-007-0408-y>
- Mitani N, Yamaji N, Ma JF.** Identification of maize silicon influx transporters. *Plant Cell Physiol.* 2009;**50**(1):5–12. <https://doi.org/10.1093/pcp/pcn110>
- Montpetit J, Vivancos J, Mitani-Ueno N, Yamaji N, Rémus-Borel W, Belzile F, Ma JF, Bélanger RR.** Cloning, functional characterization and heterologous expression of *Talsi1*, a wheat silicon transporter gene. *Plant Mol Biol.* 2012;**79**(1–2):35–46. <https://doi.org/10.1007/s11103-012-9892-3>
- Napier RM, Fowke LC, Hawes C, Lewis M, Pelham HR.** Immunological evidence that plants use both HDEL and KDEL for targeting proteins to the endoplasmic reticulum. *J Cell Sci.* 1992;**102**(2):261–271. <https://doi.org/10.1242/jcs.102.2.261>
- Naramoto S.** Polar transport in plants mediated by membrane transporters: focus on mechanisms of polar auxin transport. *Curr Opin Plant Biol.* 2017;**40**:8–14. <https://doi.org/10.1016/j.pbi.2017.06.012>
- Noronha H, Silva A, Mitani-Ueno N, Conde C, Sabir F, Prista C, Soveral G, Isenring P, Ma JF, Bélanger RR, et al.** The grapevine NIP2; 1 aquaporin is a silicon channel. *J Exp Bot.* 2020;**71**(21):6789–6798. <https://doi.org/10.1093/jxb/eraa294>
- Ramvalho JJ, Jones VAS, Mutte S, Weijers D.** Pole position: how plant cells polarize along the axes. *Plant Cell.* 2022;**34**(1):174–192. <https://doi.org/10.1093/plcell/koab203>
- Saitoh Y, Mitani-Ueno N, Saito K, Matsuki K, Huang S, Yang L, Yamaji N, Ishikita H, Shen JR, Ma JF, et al.** Structural basis for high selectivity of a rice silicon channel *Lsi1*. *Nat Commun.* 2021;**12**(1):1–14. <https://doi.org/10.1038/s41467-021-26535-x>
- Sakurai J, Ishikawa F, Yamaguchi T, Uemura M, Maeshima M.** Identification of 33 rice aquaporin genes and analysis of their expression and function. *Plant Cell Physiol.* 2005;**46**(9):1568–1577. <https://doi.org/10.1093/pcp/pci172>
- Sakurai G, Satake A, Yamaji N, Mitani-Ueno N, Yokozawa M, Feugier FG, Ma JF.** In silico simulation modeling reveals the importance of the Casparian strip for efficient silicon uptake in rice roots. *Plant Cell Physiol.* 2015;**56**(4):631–639. <https://doi.org/10.1093/pcp/pcv017>
- Sasaki A, Yamaji N, Yokosho K, Ma JF.** Nramp5 is a major transporter responsible for manganese and cadmium uptake in rice. *Plant Cell.* 2012;**24**(5):2155–2167. <https://doi.org/10.1105/tpc.112.096925>
- Shao JF, Yamaji N, Huang S, Ma JF.** Fine regulation system for distribution of boron to different tissues in rice. *New Phytol.* 2021;**230**(2):656–668. <https://doi.org/10.1111/nph.17169>
- Shao JF, Yamaji N, Liu XW, Yokosho K, Shen RF, Ma JF.** Preferential distribution of boron to developing tissues is mediated by the intrinsic protein OsNIP3. *Plant Physiol.* 2018;**176**(2):1739–1750. <https://doi.org/10.1104/pp.17.01641>
- Shimizu Y, Uemura T.** The sorting of cargo proteins in the plant *trans*-Golgi network. *Front Plant Sci.* 2022;**13**:957995. <https://doi.org/10.3389/fpls.2022.957995>
- Shiono K, Ando M, Nishiuchi S, Takahashi H, Watanabe K, Nakamura M, Matsuo Y, Yasuno N, Yamanouchi U, Fujimoto M, et al.** RCN1/OsABCG5, An ATP-binding cassette (ABC) transporter, is required for hypodermal suberization of roots in rice (*Oryza sativa*). *Plant J.* 2014;**80**(1):40–51. <https://doi.org/10.1111/tjp.12614>
- Strasser R.** Protein quality control in the endoplasmic reticulum of plants. *Annu Rev Plant Biol.* 2018;**69**(1):147. <https://doi.org/10.1146/annurev-arplant-042817-040331>
- Sun SK, Chen Y, Che J, Konishi N, Tang Z, Miller AJ, Ma JF, Zhao FJ.** Decreasing arsenic accumulation in rice by overexpressing OsNIP1; 1 and OsNIP3; 3 through disrupting arsenite radial transport in roots. *New Phytol.* 2018;**219**(2):641–653. <https://doi.org/10.1111/nph.15190>
- Sun H, Duan Y, Mitani-Ueno N, Che J, Jia J, Liu J, Guo J, Ma JF, Gong H.** Tomato roots have a functional silicon influx transporter but not a functional silicon efflux transporter. *Plant Cell Environ.* 2020;**43**(3):732–744. <https://doi.org/10.1111/pce.13679>
- Sun H, Guo J, Duan Y, Zhang T, Huo H, Gong H.** Isolation and functional characterization of *CsLsi1*, a silicon transporter gene in *Cucumis sativus*. *Physiol Plant.* 2017;**159**(2):201–214. <https://doi.org/10.1111/ppl.12515>
- Synek L, Pleskot R, Sekereš J, Serrano N, Vukašinić N, Ortmannová J, Klejchová M, Pejchar P, Batystová K, Gutkowska M, et al.** (2021) Plasma membrane phospholipid signature recruits the plant exocyst complex via the EXO70A1 subunit. *Proc Natl Acad Sci USA* **118**(36):e2105287118 <https://doi.org/10.1073/pnas.2105287118>
- Takano J, Tanaka M, Toyoda A, Miwa K, Kasai K, Fujii K, Onouchi H, Naito S, Fujiwara T.** Polar localization and degradation of *Arabidopsis* boron transporters through distinct trafficking pathways. *Proc Natl Acad Sci USA.* 2010;**107**(11):5220–5225. <https://doi.org/10.1073/pnas.0910744107>
- Tejos R, Sauer M, Vanneste S, Palacios-Gomez M, Li H, Heilmann M, van Wijk R, Vermeer JEM, Heilmann I, Munnik T, et al.** Bipolar plasma membrane distribution of phosphoinositides and their requirement for auxin-mediated cell polarity and patterning in *Arabidopsis*. *Plant Cell.* 2014;**26**(5):2114–2128. <https://doi.org/10.1105/tpc.114.126185>
- Ueno D, Sasaki A, Yamaji N, Miyaji T, Fujii Y, Takemoto Y, Moriyama S, Che J, Moriyama Y, Iwasaki K, et al.** A polarly localized transporter for efficient manganese uptake in rice. *Nat Plants.* 2015;**1**(12):1–8. <https://doi.org/10.1038/nplants.2015.170>
- Wang Z, Yamaji N, Huang S, Zhang X, Shi M, Fu S, Yang G, Ma JF, Xia J.** OsCASP1 is required for Casparian strip formation at endodermal cells of rice roots for selective uptake of mineral elements. *Plant Cell.* 2019;**31**(11):2636–2648. <https://doi.org/10.1105/tpc.19.00296>
- Wang S, Yoshinari A, Shimada T, Hara-Nishimura I, Mitani-Ueno N, Ma JF, Naito S, Takano J.** Polar localization of the NIP5; 1 boric acid channel is maintained by endocytosis and facilitates boron transport in *Arabidopsis* roots. *Plant Cell.* 2017;**29**(4):824–842. <https://doi.org/10.1105/tpc.16.00825>
- Yamaji N, Mitani N, Ma JF.** A transporter regulating silicon distribution in rice shoots. *Plant Cell.* 2008;**20**(5):1381–1389. <https://doi.org/10.1105/tpc.108.059311>
- Yoshinari A, Fujimoto M, Ueda T, Inada N, Naito S, Takano J.** DRP1-dependent endocytosis is essential for polar localization and boron-induced degradation of the borate transporter BOR1 in *Arabidopsis thaliana*. *Plant Cell Physiol.* 2016;**57**(9):1985–2000. <https://doi.org/10.1093/pcp/pcw121>
- Yoshinari A, Hosokawa T, Amano T, Beier MP, Kunieda T, Shimada T, Hara-Nishimura I, Naito S, Takano J.** Polar localization of the borate exporter BOR1 requires AP2-dependent endocytosis. *Plant Physiol.* 2019;**179**(4):1569–1580. <https://doi.org/10.1104/pp.18.01017>
- Yoshinari A, Hosokawa T, Beier MP, Oshima K, Ogino Y, Hori C, Takasuka TE, Fukao Y, Fujiwara T, Takano J.** Transport-coupled ubiquitination of the borate transporter BOR1 for its boron-dependent degradation. *Plant Cell.* 2021;**33**(2):420–438. <https://doi.org/10.1093/plcell/koaa020>
- Yoshinari A, Takano J.** Insights into the mechanisms underlying boron homeostasis in plants. *Front Plant Sci.* 2017;**8**:1951. <https://doi.org/10.3389/fpls.2017.01951>
- Zhao XQ, Mitani N, Yamaji N, Shen RF, Ma JF.** Involvement of silicon influx transporter OsNIP2; 1 in selenite uptake in rice. *Plant Physiol.* 2010;**153**(4):1871–1877. <https://doi.org/10.1104/pp.110.157867>